Transmit Correlation Diversity: Generalization, New Techniques, and Improved Bounds

Fan Zhang, Student Member, IEEE, Khac-Hoang Ngo, Member, IEEE, Sheng Yang, Member, IEEE, and Aria Nosratinia, Fellow, IEEE

Abstract-When the users in a MIMO broadcast channel experience different spatial transmit correlation matrices, a class of gains is produced that is denoted transmit correlation diversity. This idea was conceived for channels in which transmit correlation matrices have mutually exclusive eigenspaces, allowing non-interfering training and transmission. This paper broadens the scope of transmit correlation diversity to the case of partially and fully overlapping eigenspaces and introduces techniques to harvest these generalized gains. For the two-user MIMO broadcast channel, we derive achievable degrees of freedom (DoF) and achievable rate regions with/without channel state information at the receiver (CSIR). When CSIR is available, the proposed achievable DoF region is tight in some configurations of the number of receive antennas and the channel correlation ranks. We then extend the DoF results to the K-user case by analyzing the interference graph that characterizes the overlapping structure of the eigenspaces. Our achievability results employ a combination of product superposition in the common part of the eigenspaces, and pre-beamforming (rate splitting) to create multiple data streams in non-overlapping parts of the eigenspaces. Massive MIMO is a natural example in which spatially correlated link gains are likely to occur. We study the achievable downlink sum rate for a frequency-division duplex massive MIMO system under transmit correlation diversity.

Index Terms—MIMO broadcast channels, spatial correlation, channel state information, rate splitting, product superposition

I. INTRODUCTION

The effect of spatial correlation on the capacity of MIMO links has been a subject of long-standing interest. Spatial correlation arises in part from propagation environments producing stronger signal gains in some spatial directions than others, and in part from spatially dependent patterns of the antennas. The interest in spatial correlation was sharpened by its experimental validation [1], [2], and more recently by the increasing attention to higher microwave frequencies and larger number of antennas.

Shiu *et al.* [3] proposed an abstract "one-ring" model for the spatial fading correlation and its effect on the MIMO capacity. In single-user channels with channel state information at the receiver (CSIR) but no channel state information at the

Fan Zhang and Aria Nosratinia are with the University of Texas at Dallas, Texas, USA. Khac-Hoang Ngo is with Chalmers University of Technology, Gothenburg, Sweden and Sheng Yang is with CentraleSupélec, Paris-Saclay University, Gif-sur-Yvette, France.

This work was supported in part by the grants 1527598 and 1718551 from the National Science Foundation.

The material in this paper was presented in part at the IEEE International Symposium on Information Theory (ISIT), Aachen, Germany, 2017, the IEEE Information Theory Workshop (ITW), Kaohsiung, Taiwan, 2017, the IEEE International Symposium on Information Theory (ISIT), Colorado, USA, 2018, and the IEEE Information Theory Workshop (ITW), Kanazawa, Japan, 2021.

transmitter (CSIT), channel correlation can boost power but may reduce the degrees of freedom (DoF) [4], [5], thus it can be detrimental at high signal-to-noise ratio (SNR) but a boon at low SNR. Tulino et al. [6] derived analytical characterizations of the capacity of correlated MIMO channels for the large antenna array regime. Chang et al. [7] showed that channel rank deficiency due to spatial correlation lowers the diversity-multiplexing tradeoff curves from that of uncorrelated channel. Capacity bounds subject to channel estimation errors in correlated fading have been characterized [8], [9]. Dai et al. [10] used rate splitting to analyze the asymptotic sum rate of massive MIMO with non-identical spatial correlation under CSIR and imperfect CSIT assumption, and optimized the precoders of the common messages. Of the rich broader literature on MIMO spatial correlation, we are able to mention only a few representative examples [11], [12] in the interest of brevity.

The sum-rate capacity under user-specific transmit correlations with CSIR was studied in [13], [14]. Under the assumption that all users experience identical correlation, Al-Naffouri et al. [15] showed that correlation is detrimental to the sum-rate scaling of the MIMO broadcast channels under certain transmission schemes. In practice, however, users may have non-identical correlation matrices because they are not co-located [16], making it difficult to draw conclusions based on [15]. Furthermore, at higher frequencies or with large number of antennas, when spatial correlation is unavoidable, comparing capacity against a hypothetically uncorrelated channel may have limited operational impact. Instead, a more immediate question could be: how to maximize performance in the presence of spatial correlation? A useful tool for that purpose is transmit correlation diversity, i.e., leveraging the difference between the spatial correlation observed by different users in the system in the interest of exploring and exploiting economies in training and pilots.

Transmit correlation diversity was originally conceived for transmit spatial correlation matrices that have mutually exclusive eigenspaces. Under this condition, a joint spatial division multiplexing (JSDM) transmission scheme was proposed [17]–[20] that reduces the overhead needed for channel estimation. For multi-user networks with orthogonal eigenspace correlation matrices, Adhikary and Caire [21] showed that

¹The phrase *Transmit correlation diversity* is employed in a narrow sense, describing a class of gains that are related to economy of training and pilots, and have been a subject of relatively recent interest. This is in contrast with the broader set of beamforming techniques in the presence of antenna correlation, which have a longer pedigree in wireless communication.

transmit correlation helps in multi-cell network by partitioning the user spaces into clusters according to correlation. It is also known that transmit correlation benefits the sum rate in the downlink performance of a heterogeneous cellular network (HetNet) where both macro and small cells share the same spectrum [22]. Non-overlapping transmit correlation eigenspaces have also been exploited in a two-tier system where a large number of small cells are deployed under a macro cell [23].

Except for severely rank-deficient MIMO links and relatively small number of users, in most other scenarios transmit correlation matrices corresponding to different receivers have eigenspaces whose intersection is non-trivial, i.e., they experience some overlap. This creates a natural motivation to explore and understand transmit correlation diversity in the more general setting. This paper broadens the scope of correlation diversity and introduces methods to harvest correlation diversity gains under these broader channel conditions.

The main contributions of this work are summarized as follows.

- 1) We derive achievable DoF regions for the two-user broadcast channel in spatially correlated fading under the CSIR (Theorem 1) and no free CSIR (Theorem 3) assumptions. These regions are significantly larger than the time division multiple access (TDMA) region, especially when the rank of the overlap between two correlation eigenspaces is large (see Fig. 2 and Fig. 3). In the CSIR case, we also found an outer bound (Theorem 2) which shows that our achievable DoF region is tight under certain conditions.
- 2) For the two-user broadcast channel, we propose an achievable rate region for arbitrary input distribution satisfying the power constraint (Lemma 4). We characterize this rate region with an explicit input distribution based on orthogonal pilots and Gaussian data symbols. We also derive the rate achieved with product superposition (Section V-D) and a hybrid of pre-beamforming and product superposition (Section V-E). As a by-product, we find the rate achieved with pilot-based schemes for the point-to-point channel (Theorem 4), which generalizes the result of Hassibi and Hochwald [24] to correlated fading.
- 3) We derive achievable DoF regions for the -user broad-cast channel in spatially correlated fading in the presence of CSIR (Theorem 8), as well as without free CSIR under fully overlapping eigenspaces (Theorem 9), symmetrically partially overlapping eigenspaces (Theorems 10, 11) or general correlation structure (Theorem 12).
- 4) We analyze the sum rate of a massive MIMO system operating in FDD mode by investigating the pilot reduction and opportunistic additional data transmission that is made possible by spatial correlation.

For the achievability results above, we employ prebeamforming, product superposition, or a combination thereof, in the process demonstrating that these transmission techniques can harvest transmit correlation diversity gains under partiallyoverlapping eigenspaces. For the most part, our results do not require the fading to be Rayleigh; they hold for a wider class of fading such that the channel matrix has finite entropy and finite power. Early versions of the results of this paper appeared in [25]–[28].

Notation: Bold lower-case letters, e.g., denote column vectors. Bold upper-case letters, e.g. , denote matrices. The Euclidean norm is denoted by and the Frobenius . The trace, conjugate, transpose and conjugated norm transpose of are denoted and [⊤] and respectively; and denote the identity matrix and zero matrix. respectively, and the dimensions are omitted if cleared from the context: denotes the sub-matrix containing columns from to denotes the -th column; denotes respectively the column vector and row vector containing entries from to of a column vector; denotes the subspace spanned by the columns of a truncated unitary matrix and denotes the subspace that is orthogonal to is a diagonal matrix with diagonal entries is the indicator function of event ; 1 Logarithms are in base . All rates are measured in bits per channel use.

II. SYSTEM MODEL

Consider a MIMO broadcast channel in which a transmitter (also called as base station) equipped with antennas transmitting to receivers (also called as users), where User is equipped with antennas, . The received signal at User at channel use is

$$\mathbf{H}$$
 for (1)

where is the transmitted signal at channel use and is the white noise with independent and identically distributed (i.i.d.) \mathcal{CN} entries. \mathbf{H} is the channel matrix containing the random fading coefficients between transmit antennas of the base station and receive antennas of User . We assume that \mathbf{H}

. The transmitted signal is subject to the power constraint

$$-$$
 (2)

where is the number of channel uses spanned by a codeword (of a channel code). Therefore, is the ratio between the average transmit power per antenna and the noise power, and is referred to as the SNR of the channel. Hereafter, we omit the channel use index .

1) Channel Correlation: We assume that the channel is spatially correlated according to the Kronecker model (a.k.a. separable model), and focus on the transmit-side correlation. Thus the channel matrices are expressed as

$$\mathbf{H} \quad \mathbf{H} \quad \overline{} \tag{3}$$

where $-\mathbf{H}^H\mathbf{H}$, , is the transmit correlation matrix of User with rank , and \mathbf{H}

is drawn from a generic distribution satisfying the conditions

$$\mathbf{H} \qquad \qquad \mathbf{H}^{\mathsf{H}}\mathbf{H} \tag{4}$$

Since the correlation matrices might be rank-deficient, ${\bf H}$ is not necessarily a minimal representation of the randomness in ${\bf H}$. The correlation eigenspace of User—is revealed via eigendecomposition of the correlation matrix:

where is a diagonal matrix containing non-zero eigenvalues of , and is a matrix whose orthonormal unit column vectors are the eigenvectors of corresponding to the non-zero eigenvalues. The rows of ${\bf H}$ belong to the -dimensional eigenspace of , also called as the eigenspace of User .

The channel expression (3) can be expanded as

$$\mathbf{H} \quad \mathbf{H} \quad \mathbf{H} \quad \mathbf{H} \quad \mathbf{G}$$

where \mathbf{H} is equivalently drawn from a generic distribution satisfying ,

The eigenspaces have a prominent role in transmit correlation diversity. For example, methods such as [17]–[20] are critically dependent on finding groups of users whose eigenspaces have no intersection. In contrast, in this paper, we propose transmission schemes that take advantage of both common and non-common parts of the eigenspaces. To this end, in several instances, we build an equivalent channel **H** that resides in a *subspace* of the eigenspace via the linear transformation

$$\mathbf{H} \quad \mathbf{H}$$
 (7)

for some truncated unitary matrix , , such that . Unlike , , that characterize the correlation eigenspaces of the links, the subspaces also depend on the proposed transmission schemes and may be customized throughout the paper.

2) Channel Information Availability: We assume throughout the paper that the distribution of \mathbf{H} , in particular the second-order statistic (and thus and), is known to both the base station and User . This is reasonable because represents long-term behavior of the channel that is stable and can be easily tracked. On the other hand, the realization of \mathbf{H} changes much more rapidly. We consider two scenarios:

CSIR (channel state information at the receiver): User knows perfectly the realizations of \mathbf{H} .

No free CSIR: User only knows the distribution of **H**. In this case, for a tractable model of the channel variation, we assume a block fading model with equal-length and synchronous coherence interval (across the users) of channel uses. That is, **H** remains constant during each block of length and changes independently across blocks [29]. We assume that . Let

be the transmitted signal during a block, the received signal at User during this block is

where , and the block index is omitted for simplicity. User might attempt to estimate **H** with the help of known pilot symbols inserted in .

3) Achievable Rate and DoF: Assuming independent messages are communicated (no common message), and the corresponding rate tuple is achievable at SNR, i.e., lie within the capacity region of the channel, then an achievable DoF tuple is defined as

The set of achievable rate (resp., DoF) tuples defines an achievable rate (resp., DoF) region of the channel.

For convenience, we denote

III. Preliminaries and Useful Results

Lemma 1 (The optimal single-user DoF). For the correlated MIMO broadcast channel in Section II-1, the optimal single-user DoF of User is with CSIR and

without free CSIR.

The result in the CSIR case is well-known (see, e.g., [30]). The no free CSIR case was reported in [25, Thm. 1]. The next lemma is used for the finite-SNR rate analysis.

Lemma 2 (Worst case uncorrelated additive noise [24]). *Consider the point-to-point channel*

where the channel is known to the receiver, and the signal and the noise satisfy the power constraints — and — , are both complex Gaussian distributed, and are uncorrelated, i.e, $^{\rm H}$. Let $_{\rm X}$ $^{\rm H}$ and $_{\rm W}$ $^{\rm H}$ and assume $_{\rm X}$ and $_{\rm W}$. Then the mutual information is lower bounded as

If the distribution of is left rotationally invariant, i.e., for any deterministic unitary matrix , then the minimizing noise covariance matrix in (12) is

Proof. The proof follows from the proof of [24, Thm. 1]. Specifically, the mutual information lower bound (11) was stated in [24, Eq. (27)]. To show that $_{\mathbf{w}}$, we diagonalize $_{\mathbf{w}}$ using the left rotational invariance of $_{\mathbf{w}}$, and then use the convexity of $_{\mathbf{w}}$ $_{\mathbf{w}}$ $_{\mathbf{w}}$ $_{\mathbf{w}}$ in the diagonalized $_{\mathbf{w}}$.

The next lemma gives the MMSE estimator used for pilot-based channel estimation without free CSIR.

Lemma 3 (MMSE estimator). *Consider the following linear model*

(13)

where has correlation matrix — $^{\rm H}$ is known, and has i.i.d. \mathcal{CN} entries. The linear MMSE estimator for is given by

н н (14)

The MMSE estimate is also the conditional mean:

. The estimate and the estimation error are uncorrelated, have zero mean and row covariance

H
 H H (15)

H
 H (16)

Proof. The linear MMSE channel estimator is given by where is the minimizer of the MSE

н н н

(17)

Solving \overline{A} — yields the optimal \overline{A} . Some further simple manipulations give (15) and (16). \Box

In the following, we introduce two main building blocks of our proposed achievable schemes.

A. Rate Splitting and Precoder Design

To illustrate the basic idea of rate splitting, we take a two-user broadcast for example. Define \
. Let be the precoding matrix. The transmitted signal is

(18)

Each of the signals contains an information-carrying matrix. The precoder matrices are designed satisfying the following properties:

(19)

(20) (21)

This property ensures that the receiver only sees the signal that transmit along the directions which are not orthogonal to its eigendirections. In this case, it indicates that receiver 1 can see and , while receiver 2 can see and . The precoder can be calculated from and using, e.g., the Zassenhaus algorithm [31]. Specifically, this algorithm uses elementary row operations to transform the

form ^T, where stands for a matrix which is not of interest. The precoders and can be found similarly by

applying the Zassenhaus algorithm to and , and and , respectively, where is the matrix such that is unitary.

Rate splitting has been used for precoded downlink transmission in e.g., [10], [32], [33]. Especially, in [10], the precoders are adjusted according to the non-identical spatial correlation between the users. However, these works assume that perfect CSIR and imperfect/partial CSIT are available. In our work, we design rate splitting schemes for the non-coherent setting where neither the transmitter nor the users knows the instantaneous CSI. In this case, as opposed to [10], the transmitter can only rely on the statistical CSI to design the precoders. Furthermore, pilot symbols need to be inserted and carefully aligned between eigen-subspaces for the receivers to estimate the effective channels while the pilot overhead is minimized.

B. Product Superposition

In [34], [35], Li and Nosratinia studied a two-receiver broadcast one static receiver has non-identical coherence times and proposed a product superposition scheme. In the earlier work of [25], the product superposition scheme was implemented in a two-receiver broadcast channel when two receivers have non-identical transmit correlation. Assume a two-user broadcast channel has one receiver with uncorrelated channel and the other receiver with rank-deficient correlated channel with rank , to apply product superposition, the transmitter sends the signal

where

(23)

contains symbol intended for User 1, is designed to guarantee that is non-singular, and includes symbol intended for Receiver 2. The received signal at User 1 is

$$\mathbf{H}$$
 (24)

where **H H** . Receiver 1 estimates the equivalent channel **H** and decodes , achieving degrees of freedom. The received signal at Receiver 2, during the first time slots, is

$$\overline{\mathbf{H}}$$
 (25)

where **H H** . Using the first columns, Receiver 2 estimates the channel, **H** , and furthermore using the remaining columns, Receiver 2 decodes the symbols, achieving degrees of freedom.

IV. TWO-USER BROADCAST CHANNEL: DOF ANALYSIS

Both with or without free CSIR assumption, we study first the special case of fully overlapping correlation eigenspaces, then the more general case of partially overlapping correlation eigenspaces.

A. CSIR

Consider the case where both users have spatially correlated channels, and User 's channel eigenspace is a subspace of User 's, which implies .

Proposition 1. For the two-user broadcast channel with CSIR, when the eigenspace of User is a subspace of User 's (implying), the DoF pairs , and are achievable. Furthermore, if , the DoF pair is also achievable. The convex hull of these pairs and the origin is an achievable DoF region.

The proof is available in [36] and is omitted here for brevity.

Theorem 1. For the two-user broadcast channel with CSIR and , the DoF pairs , and are achievable. Furthermore, if and , the DoF pairs

(26)

(27)

(28)

are also achievable. The convex hull of these pairs and the origin is an achievable DoF region.

The proof is available in [36] and is omitted here for brevity. An outer bound for the achievable DoF region is given as follows.

Theorem 2. When the achievable DoF region is outer bounded by , and

When or

this outer bound is tight.

The proof is available in [36] and is omitted here for brevity. Fig. 1 shows the regions where the outer bound in Theorem 2 is tight.

Fig. 2 compares the achievable region proposed in Theorem 1 and the achievable region achieved with TDMA (time sharing between and) for , , and , . The proposed achievable region is much larger than the TDMA region, especially when is small. In this setting, according to Theorem 2, the proposed region is optimal.

B. No free CSIR

In this case, CSIR is not available a priori and must be acquired via pilot transmission. On the one hand, one needs to take into account the cost of CSI acquisition in both energy and DoF. On the other hand, pilot transmission enables product superposition [34] that can improve upon rate splitting.

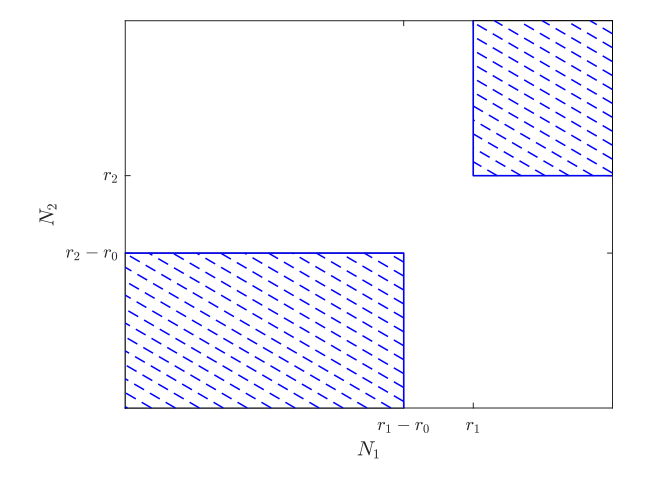


Fig. 1. Regions (the hashed part) where the outer bound for the DoF region with CSIR in Theorem 2 is tight.

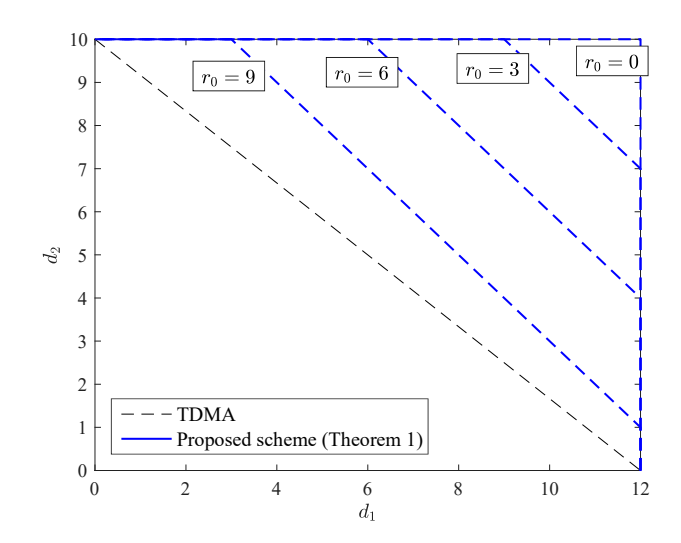


Fig. 2. The achievable DoF region for two-users with CSIR, under TDMA and the proposed scheme (Theorem 1) for , , , and , . In this case, the latter region is optimal.

1) Fully Overlapping Eigenspaces: Consider the case where User 's eigenspace is a subspace of User 's, which implies . The following proposition presents achievable DoF with product superposition in this case.

Proposition 2. In a two-user broadcast channel without free CSIR, when the eigenspace of User is a subspace of User 's (implying), the DoF pair — is achievable with product superposition.

Proof. There exist transmit eigendirections and that are aligned with the non-common and common parts, respectively, of the two channel eigenspaces such that

(29)

\ (30)

Define . Let the transmitter send the signal

during a coherence block, with	
and , where	(39)
contains symbols for User and contains symbols for User . The received signal at User is	\mathcal{D} ——
$\mathbf{H} \qquad \qquad \mathbf{H} \tag{31}$	
User estimates the equivalent channel H and then decodes , achieving DoF. The received signal at User during the first channel uses is	are achievable. The convex hull of these DoF pairs (over all feasible values of , and) and the origin is achievable.
	Remark 1. The parameters represent the allocation
using H due to (30). User estimates the equivalent channel H , and then decodes , achieving DoF. Therefore, the normalized DoF pair — ——————————————————————————————————	of available dimensions to encoding of messages for the two users. By tuning these parameters, we explore the trade-off between the number of data dimensions (indicating the amount of channel uses needed for pilot transmission) and the amount of channel uses for data transmission within each section of the eigenspaces.
2) Partially Overlapping Eigenspaces:	Proof of Theorem 3. The DoF pairs — and
Theorem 3. For the two-user broadcast channel without free CSIR and , the DoF pairs — and — are achievable. Furthermore, for any integers , , and , the DoF pairs D — (33) D — (33)	— are achieved by activating only one user according to Lemma 1. For any non-negative integers satisfying , and , there exist eigendirections , such that User 1 can only see signals in the direction of and , while User 2 can only see signals in the direction of and . (See Section III-A.) To achieve $\mathcal D$, the base station employs product superposition and transmits
(34)	(41)
are achievable. On top of that, if , the DoF pairs	with and where
\mathcal{D} (35) \mathcal{D} (36)	and contain symbols for User and User , respectively. Following steps similar to the proof of Proposition 2, it can be shown that this achieves the DoF pair $\mathcal D$. The DoF pair $\mathcal D$ can be achieved similarly by switching the users' role. When , the pairs $\mathcal D$ and $\mathcal D$ are achieved with rate splitting as follows. Let the transmitter send
D	(42)
are achievable; if , the DoF pairs D ——— (37)	where is a common signal to both users while and are private signals to User and User , respectively. The received signal at User is
	$\mathbf{H} \tag{43}$
$\mathcal{D} \tag{38}$	User estimates the equivalent channel H during the first channel uses and decodes both and during the remaining channel uses, achieving

——— DoF. The received signal at User

is

H

(44)

User estimates the equivalent channel \mathbf{H} and then decodes and , achieving — DoF. By dedicating to only User or User , DoF pairs \mathcal{D} and \mathcal{D} are achieved, respectively.

The degrees of freedom pair \mathcal{D} can be achieved (still assuming), via a combination of rate splitting and product superposition as follows. The transmitted signal is

(45)

with , , and , where con-

tains symbols intended for User while and contain symbols intended for User . The received signal at User is

 \mathbf{H} (46)

User estimates the equivalent channel ${\bf H}$, and then decodes to achieve — DoF. The received signal at User is

 $\mathbf{H} \tag{47}$

where . User estimates its equivalent channel \mathbf{H} in the first channel uses, and then decodes and , achieving —— DoF in total. Therefore, \mathcal{D} is achieved. Therefore, the proof for the case where A similar analysis applies to the case the proof of Theorem 3.

In Figure 3, the achievable DoF region in Theorem 3 is shown for the scenario where , , , and . Similar to the CSIR case, exploiting the channel correlation improves significantly the DoF region upon TDMA, especially for small . Note that TDMA was shown to be degrees of freedom optimal when the channel is uncorrelated [37].

This completes the DoF analysis for the two-user case. By using both product superposition and rate splitting, achievable DoF regions were calculated for a variety of correlation structures and antenna configurations. Also, an outer bound was calculated under perfect CSIR.

V. TWO-USER BROADCAST CHANNEL: RATE ANALYSIS

We assume no free CSIR under partially overlapping eigenspaces, and assume that , . In addition, without loss of generality .

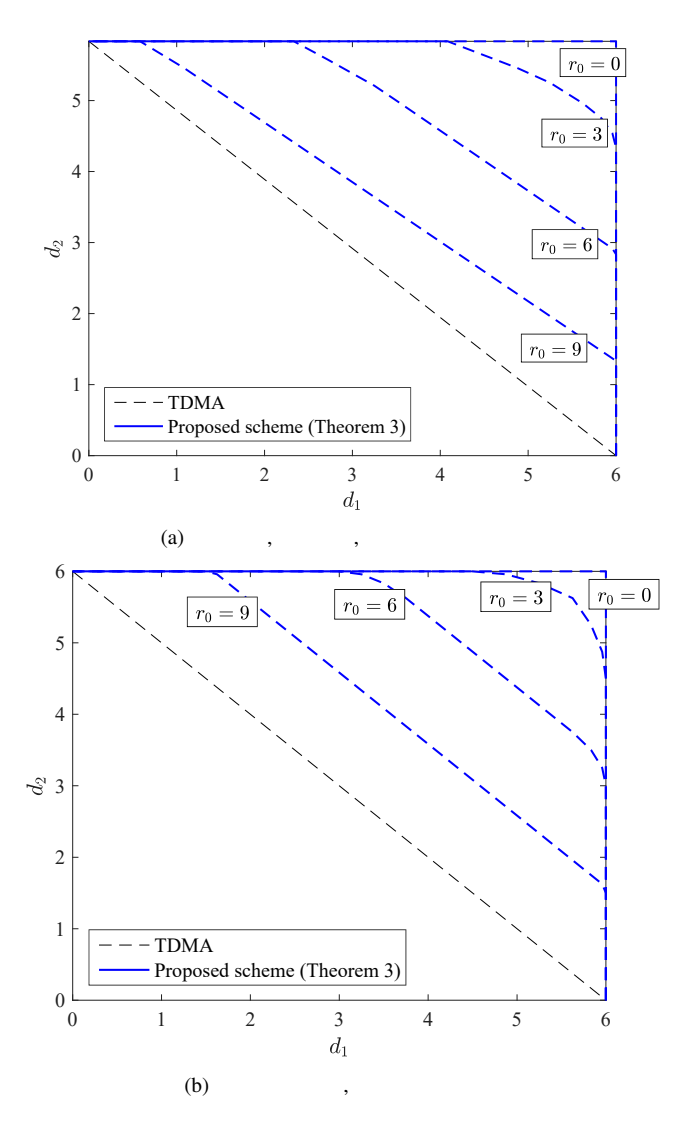


Fig. 3. The DoF region for the two-user broadcast channel without free CSIR, achieved with TDMA or the proposed scheme (Theorem 3) for , and

A. The Single-User Case

Let us first consider the single-user case where, for simplicity, we omit the user's index. The received signal is

(48)

where the assumptions for the transmitted signal , the Gaussian noise , and the channel are as before. In particular, is block fading with coherence time , and has correlation matrix

H, thus can be written as

H with

H drawn from a generic distribution. The following theorem states the achievable rate (in bits/channel use) for this channel.

Theorem 4. Achievable rates for a single-user spatially-correlated MIMO channel without free CSIR are as follows.

1) if the transmitter does not know the channel correlation matrix ,

н	н
(49)	(54
where rows of are i.i.d. according to \mathcal{CN} , and ;	where rows of are i.i.d. according to \mathcal{CN} , and ;
2) if the transmitter knows the channel correlation matrix , under orthogonal pilots:	If the base station transmits in the eigenspace of using precoder , i.e., H, and optimizes the pilot the following corollary demonstrates the achievable rate:
н	Corollary 3. For 2-user broadcast channel, when the transmitter emits in the eigenspace of , the following single-user rate is achievable:
where rows of are i.i.d. according to \mathbb{CN} such that H for a truncated unitary matrix such that . Allowing non-orthogonal pilots can improve the rate to:	H
— н	where rows of are i.i.d. according to \mathcal{CN} , and . A
(51)	corresponding (single-user) rate applies for The optimal power allocation for (55) closely follows: Remark 2 and is ommitted for brevity. The convex hull of
where rows of $\ \ \ \ \ \ \ \ \ \ \ \ \ \ \ \ \ \ \$, and is achievable by TDMA.
	C. Rate Splitting In the following, we analyze the rate achievable with the
Proof. See Appendix A. Remark 2. The optimal power allocation for the rate in (51) is given by ———————————————————————————————————	schemes achieving the DoF region in Theorem 3. Recall that for a set of non-negative integers , , and , the precoding matrices in Section III-A, define H , H , H , (So);
where R and R	н , н , н (so
Corollary 1. If the channel is uncorrelated, i.e., , the achievable rate is	Let the base station transmit
н	(56)
where is the uncorrelated channel matrix. This coincides with [24, Eq.(21)].	where , , and are independent and satisfy the powe constraint . Thanks to the precoders, the private signal is seen by User only while the common signal is seen by both users. The received signals become
B. The Baseline TDMA Schemes	(57)
We consider TDMA without free CSIR. If only User is activated and the base station does not exploit , according to Theorem 4, the following corollary demonstrates the achievable rate:	where the equivalent channels and are correlated and unknown
Corollary 2. For 2-user broadcast channel, when the transmitter does not know channel correlations , the following single-user rates are achievable for users :	It can be observed that the received signal at each user is similar to a non-coherent two-user MAC: (57) as the MAC with () equivalent transmit antennas and receive antennas (58) as the MAC with () equivalent transmit antennas

and

signal

receive antennas. The two MACs share a common

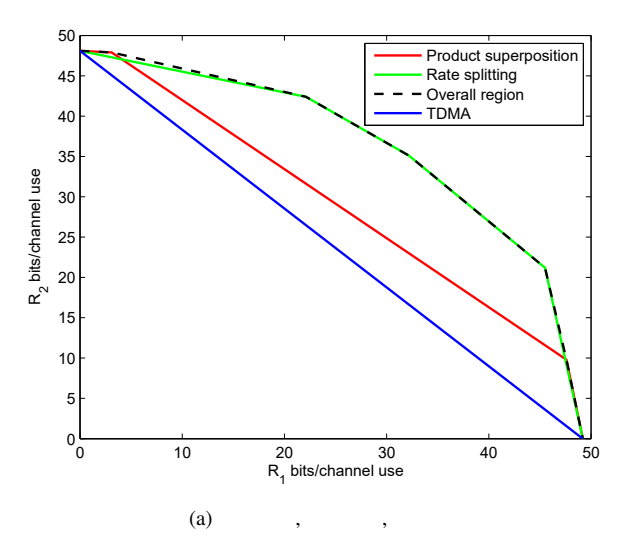
Component powers and solity in the region can be achieved in the rowser correlated broadcast channel with partially overlapped eigenspaces: Component powers are where the manual information terms in Lemma 4, we have the following theorem: Component powers are whith private signal user 2 achieves rate with private signal user 3 achievable with:	From the capacity region of multiple access channels [38], we know that the rate pairs and are simultaneously achievable for the MAC and MAC, respectively, if the rates satisfy	н н (72)
where rows of obey CN and are independent of each other. (62) (63) (64) Then, User achieves rate with private signal users can achieve rate with common signal Let be the User's share in the rate pair is achievable. Replacing is achievable. Replacing is achievable. Replacing is achievable. Replacing is achievable with: Lemma 4. With rate splitting and without free CSIR. rate pairs are achievable with: (65) By bounding the mutual information terms in Lemma 4, we have the following theorem: Theorem 5. Under rate splitting, the following rate region can be achieved in the two-user correlated broadcast channel with partially overlapped eigenspaces: (68) (69) (70) The overall achievable rate region is the convex hull of (68) (69) and (70) over all feasible values of and power allocations (77). Proof. Sec Appendix B. D. Product Superposition, the following rate rate of the product superposition, the following rate of the product superposition, the following rate rate region to the following rate. Theorem 6. With product superposition, the following rate. Theorem 6. With product superposition, the following rate.	– (59)	н н
and are independent of each other. (62) (63) (64) Then, User achieves rate with private signal user 2 achieves rate with private signal and both users can achieve rate with common signal Let be the User 's share in then the rate pair is achievable. Replacing and in (59)-(64) and applying Fourier-Motzkin elimination leads to the following result. Lemma 4. With rate splitting and without free CSIR, rate pairs are achievable with: (65) (67) (67) (68) (69) Theorem 5. Under rate splitting, the following rate region can be achieved in the two-user correlated broadcast channel with partially overlapped eigenspaces: (68) (69) (70) Where Theorem 6. With product superposition, the following rate region is call feasible values of and power allocations (77). Proof. See Appendix B. D. Product Superposition, the following rate region to the convex hull of (68) and (70) over all feasible values of and power allocations (77). Theorem 6. With product superposition, the following rate region to the convex hull of (68) and (70) over all feasible values of and power allocations (77). Theorem 6. With product superposition, the following rate region to the convex hull of (68). (71)	- (60)	(73)
Then, User achieves rate with private signal user 2 achieves rate with private signal user 2 achieves rate with private signal user 3 achieves rate with private signal user 4 achieves rate with common signal user 5 achieves rate with common signal user 6 achieves rate with common signal user 7 achieves rate with common signal user 8 achievable. Replacing and in (59)-(64) and applying 8 are achievable with: Common 4 With rate splitting and without free CSIR, rate pairs are achievable with: Common 5 under rate splitting, the following rate region can be achieved in the two-user correlated broadcast channel with partially overlapped eigenspaces: Common 5 under rate splitting, the following rate region can be achieved in the two-user correlated broadcast channel with partially overlapped eigenspaces: Common 5 under rate splitting, the following rate region can be achieved in the two-user correlated broadcast channel with partially overlapped eigenspaces: Common 5 under rate splitting, the following rate region can be achieved in the two-user correlated broadcast channel with partially overlapped eigenspaces: Common 5 under rate splitting, the following rate region can be achieved in the two-user correlated broadcast channel with partially overlapped eigenspaces: Common 5 under rate splitting, the following rate region can be achieved in the two-user correlated broadcast channel with partially overlapped eigenspaces: Common 5 under rate splitting, the following rate region can be achieved in the two-user correlated broadcast channel with partially overlapped eigenspaces: Common 5 under rate splitting, the following rate region can be achieved in the two-user correlated broadcast channel with partially overlapped eigenspaces: Common 5 under rate splitting, the following rate region can be achieved by the power constraint Common can be achieved by the	- (61)	
Then, User achieves rate with private signal , and both users can achieve rate with private signal , and both users is achievable. Replacing , and in (59)-(64) and applying Fourier-Motzkin elimination leads to the following result. Lemma 4. With rate splitting and without free CSIR, rate pairs are achievable with: (65) (66) (67) For input distributions , and satisfying about the following the mutual information terms in Lemma 4, we have the following theorem: Theorem 5. Under rate splitting, the following rate region can be achieved in the two-user correlated broadcast channel with partially overlapped eigenspaces: (68) (69) (70) (71) The overall achievable values of and power allocations (77). Proof. See Appendix B. D. Product Superposition, the following rate redion. Theorem 6. With product superposition, the following rate redion. Theorem 6. With product superposition, the following rate redion. Theorem 6. With product superposition, the following rate redion. Theorem 6. With product superposition, the following rate redion. Theorem 6. With product superposition, the following rate rate.	- (62)	and are independent of each other.
Then, User achieves rate with private signal , and both users can achieve rate with private signal , and both users is achievable. Replacing , and in (59)-(64) and applying Fourier-Motzkin elimination leads to the following result. Lemma 4. With rate splitting and without free CSIR, rate pairs are achievable with: (65) (66) (67) For input distributions , and satisfying about the following the mutual information terms in Lemma 4, we have the following theorem: Theorem 5. Under rate splitting, the following rate region can be achieved in the two-user correlated broadcast channel with partially overlapped eigenspaces: (68) (69) (70) (71) The overall achievable values of and power allocations (77). Proof. See Appendix B. D. Product Superposition, the following rate redion. Theorem 6. With product superposition, the following rate redion. Theorem 6. With product superposition, the following rate redion. Theorem 6. With product superposition, the following rate redion. Theorem 6. With product superposition, the following rate redion. Theorem 6. With product superposition, the following rate rate.	- (63)	
Then, User achieves rate with private signal , user 2 achieves rate with private signal , and both users can achieve rate with common signal . Let be the User 's share in , then the rate pair is achievable. Replacing and in (59)-(64) and applying Fourier-Motkin elimination leads to the following result. Lemma 4. With rate splitting and without free CSIR, rate pairs are achievable with: - (65) - (67) For input distributions , and satisfying where rows of are i.i.d. according to CN Variables allocate degrees of freedom and satisfy and satisfy the power constraint Theorem 5. Under rate splitting, the following rate region can be achieved in the two-user correlated broadcast channel with partially overlapped eigenspaces: (68) (69) (70) The overall achievable rate region is the convex hull of (68) (69) and (70) over all feasible values of and power allocations (77). Proof. See Appendix B. D. Product Superposition, the following rate rate on the following rate region is the convex following rate region is the convex hull of (68) (69) and (70) over all feasible values of and power allocations (77). Proof. See Appendix B.		
pairs are achievable with: - (65) - (75) - (75) - (75) - (76) - (77) -	2 achieves rate with private signal , and both users can achieve rate with common signal . Let be the User 's share in , then the rate pair is achievable. Replacing , and in (59)-(64) and applying	———
(66) (67) (68) (69) The overall achievable rate region is the convex hull of (68), (69) and (70) over all feasible values of and power allocations (77). Where (68) (69) The overall achievable rate region is the convex hull of (68), (69) and (70) over all feasible values of and power allocations (77). Proof. See Appendix B. (71) (75) (66) (67) (67) (67) (68) (77) (78) (79) (70) (70) (71) (71) (71) (71) (72) (72) (73) (74) (75) (75) (76) (76) (77) (77) (77) (78) (79) (79) (70) (70) (71) (71) (71) (71) (71) (72) (73) (74) (75) (75)		
(66) (67) (68) (69) The overall achievable rate region is the convex hull of (68), (69) and (70) over all feasible values of and power allocations (77). Where (68) (69) The overall achievable rate region is the convex hull of (68), (69) and (70) over all feasible values of and power allocations (77). Proof. See Appendix B. (71) (75) (66) (67) (67) (67) (68) (77) (78) (79) (70) (70) (71) (71) (71) (71) (72) (72) (73) (74) (75) (75) (76) (76) (77) (77) (77) (78) (79) (79) (70) (70) (71) (71) (71) (71) (71) (72) (73) (74) (75) (75)	_	
(66) (67) (67) (67) (67) (67) (68) By bounding the mutual information terms in Lemma 4, we have the following theorem: Theorem 5. Under rate splitting, the following rate region can be achieved in the two-user correlated broadcast channel with partially overlapped eigenspaces: (68) (69) (70) (69) (70) (69) (70) (69) (70) (71) The overall achievable rate region is the convex hull of (68), (69) and (70) over all feasible values of and power allocations (77). Proof. See Appendix B. D. Product Superposition, the following rate and satisfy the power constraint.	(65)	
for input distributions , , and satisfying By bounding the mutual information terms in Lemma 4, we have the following theorem: Theorem 5. Under rate splitting, the following rate region can be achieved in the two-user correlated broadcast channel with partially overlapped eigenspaces: (68) (69) (70) The overall achievable rate region is the convex hull of (68) (69) and (70) over all feasible values of and power allocations (77). Proof. See Appendix B. D. Product Superposition, the following rate region is the following rate of an and power allocations, the following rate of the product superposition, the following rate of the product superposition of the product superposition the product superposition of the product	(66)	
for input distributions , , and satisfying	_	
for input distributions , , and satisfying where rows of are i.i.d. according to CN Variables allocate degrees of freedom and satisfy and The component powers satisfy the power constraint satisfy the power constraint with partially overlapped eigenspaces: (68) (69) (70) Where rows of are i.i.d. according to CN Variables allocate degrees of freedom and satisfy and The component powers satisfy the power constraint. (68) (69) (70) The overall achievable rate region is the convex hull of (68), (69) and (70) over all feasible values of and power allocations (77). Proof. See Appendix B	(67)	
By bounding the mutual information terms in Lemma 4, we have the following theorem: Theorem 5. Under rate splitting, the following rate region can be achieved in the two-user correlated broadcast channel with partially overlapped eigenspaces: (68) (69) (70) Wariables allocate degrees of freedom and satisfy and The component powers satisfy the power constraint The overall achievable rate region is the convex hull of (68), (69) and (70) over all feasible values of allocations (77). Proof. See Appendix B. D. Product Superposition Theorem 6. With product superposition, the following rate	for input distributions , , and satisfying	
can be achieved in the two-user correlated broadcast channel with partially overlapped eigenspaces: (68) (77) (69) (70) The overall achievable rate region is the convex hull of (68), (69) and (70) over all feasible values of and power allocations (77). Proof. See Appendix B. D. Product Superposition Theorem 6. With product superposition, the following rate	•	\mathcal{CN} Variables allocate degrees of freedom and satisfy ,
where (69) (70) The overall achievable rate region is the convex hull of (68), (69) and (70) over all feasible values of and power allocations (77). Proof. See Appendix B. D. Product Superposition Theorem 6. With product superposition, the following rate	can be achieved in the two-user correlated broadcast channel	satisfy the power constraint
The overall achievable rate region is the convex hull of (68), (69) and (70) over all feasible values of and power allocations (77). Proof. See Appendix B. D. Product Superposition Theorem 6. With product superposition, the following rate	(68)	(77)
where (69) and (70) over all feasible values of and power allocations (77). Proof. See Appendix B. D. Product Superposition Theorem 6. With product superposition, the following rate	(69)	The overall achievable rate recion is the convex bull of (69)
D. Product Superposition Theorem 6. With product superposition, the following rate		(69) and (70) over all feasible values of and power
Theorem 6. With product superposition, the following rate		<i>Proof.</i> See Appendix B.
Theorem 6. With product superposition, the following rate		D. Product Superposition
	——————————————————————————————————————	Theorem 6. With product superposition, the following rate

— (78)		
where rows of are i.i.d. according to \mathcal{CN} ;		
(79)	н	
where rows of are i.i.d., zero mean, with covariance , where	———	
— н	——— н (84)	
allocate degrees of freedom to signal components, and satisfy and with the power constraint ———— (81)	where rows of are i.i.d. according to \mathcal{CN} H and rows of are i.i.d. according to \mathcal{CN} , and they are independent of each other. Variables allocate degrees of freedom to signal components, and satisfy , and with the power constraint	
By swapping the users' role, another achievable rate pair is obtained. The overall achievable rate region is the convex hull of these pairs over all feasible values of and feasible power allocations (81).	(85) The overall achievable rate region is the convex hull of these	
Remark 3. The distribution of is non-Gaussian. As	pairs over power allocations satisfying the power constraint and all feasible values of .	
clarified in (262), it consists of a Gaussian matrix plus the product of two other Gaussian matrices. Proof. See Appendix C.	Remark 4. The distribution of is non-Gaussian. As clarified in (274), it consists of a Gaussian matrix plus the product of two other Gaussian matrices.	
	<i>Proof.</i> See the Appendix D. \Box	
 E. Hybrid Superposition Hybrid superposition in this paper refers to a composite scheme that involves both rate splitting and product superposition. Theorem 7. With hybrid superposition, the following rate pair 	Remark 5. Hybrid superposition utilizes both rate splitting and product superposition but is not a generalization, in the sense that the results of pure rate splitting and product superposition cannot be recovered from the hybrid scheme. At very high SNR under partially overlapped eigenspaces, hybrid superposition	
can be achieved:	can improve over rate splitting and product superposition, but in other channel conditions, the hybrid superposition may in fact perform worse than the individual schemes.	
——————————————————————————————————————	F. Numerical Results	
where rows of are i.i.d., zero mean, with covariance , where	Simulations in this section assume Rayleigh fading, i.e., has independent \mathcal{CN} entries. The correlation matrix H, is generated by assuming the same magnitude along all eigendirections, i.e., Furthermore, we assume the eigendirections of transmit correlation matrices of the two users are either the same or orthogonal to each	
— н	other. The simplicity of this configuration makes it suitable for a representative example. Assuming a constant magnitude along different eigendirections allows us to concentrate on	

e.g., water-filling.

and

gains that are *purely* due to correlation diversity rather than,



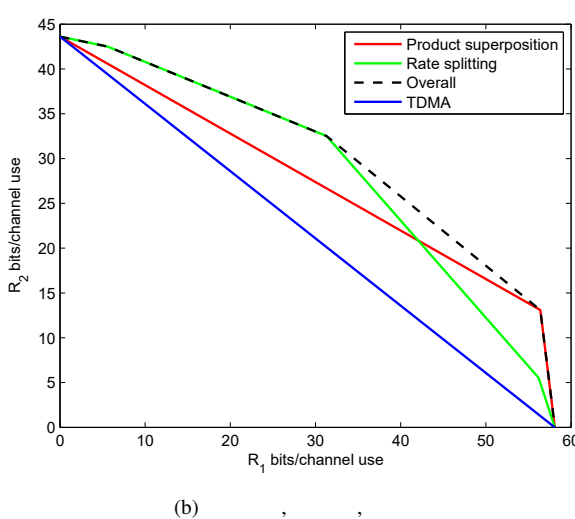


Fig. 4. The rate regions of various schemes for the spatially correlated broadcast channel $$\operatorname{\textsc{d}B}$.$

When the eigenspaces of the two users are partially overlapped, in Fig. 4, we plot the rate regions achieved with these schemes in a setting of , , , ,

We observe that the performance of rate splitting and product superposition depends strongly on the rank of the eigenspaces. When the rank of the two individual eigenspaces is close to each other, rate splitting will obtain a better rate region since the gains achieved by product superposition come from the difference between the rank of the two eigenspaces. In the channel configuration in Fig. 4, the hybrid superposition scheme produced rates that are inferior to both product superposition and to rate splitting, therefore they are not displayed. Hybrid superposition becomes competitive at very high SNR, while the results of this section focus on moderate SNR.

When one of the users' eigenspace is strictly a subspace of the other, rate splitting performs no better than TDMA. We plot the rate region for this scenario achieved via product superposition in a setting of , , ,

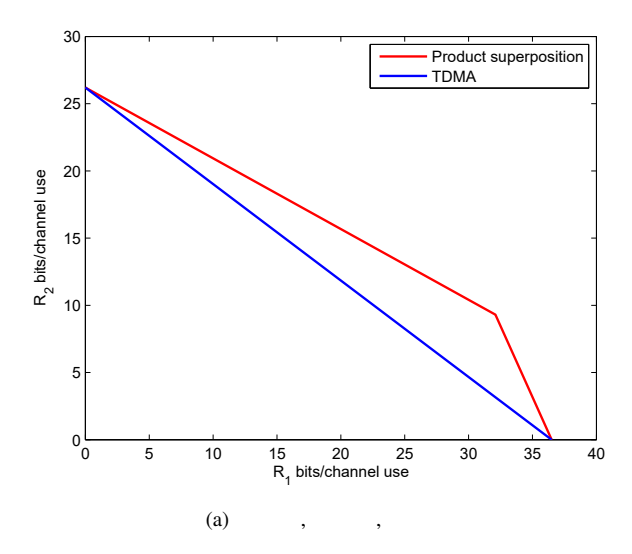


Fig. 5. The rate region of

and at power constraint dB.

VI. -USER BROADCAST CHANNEL: DOF ANALYSIS

To extend the study to the $\,$ -user scenario, some further assumptions on the correlation model are made as follows. Recall that the rows of H belong to the eigenspace of $\,$.

Denote the sum of all channel eigenspaces as follows²

$$V$$
 (86)

Define $\mathcal{V}_{\mathcal{J}}$ \mathcal{J} \mathcal{J} , for \mathcal{J} , and \mathcal{V} $\mathcal{V}_{\mathcal{J}}$ \mathcal{J} \mathcal{J} \mathcal{J} , . . . Define \mathcal{J} $\mathcal{V}_{\mathcal{J}}$. Obviously, \mathcal{J} \mathcal{J} \mathcal{J} \mathcal{J} . Therefore, we can generate subspaces $\mathcal{V}_{\mathcal{J}}$ of \mathcal{J} dimensional whose \mathcal{J} basis vectors span the channel of every user in a non-empty group \mathcal{J} and are linear independent to all vectors in for \mathcal{J} . An example of the correlation structure for the case of three-user broadcast channel is shown in Fig. 6.

In this way, the signal transmitted in the subspace $\mathcal{V}_{\mathcal{J}}$ can be seen by every user in \mathcal{J} and is vague to all other users. On the other hand, the signals transmitted in $\mathcal{V}_{\mathcal{J}}$ and $\mathcal{V}_{\mathcal{K}}$ interfere each other at every user in $\mathcal{J} \setminus \mathcal{K}$. To characterize the interfering relation between signals transmitted in different subspaces, we introduce the concept of *interference graph* as follows:

Definition 1. For , the interference graph of order , denoted by , is an undirected graph for which:

the set of vertices is the set of unordered subsets of cardinality of , i.e., \mathcal{J} \mathcal{J} , hence a vertex is also denoted by a subset \mathcal{J} ;

there exists an edge between two vertices $\mathcal J$ and $\mathcal K$ if and only if $\mathcal J\setminus\mathcal K$

 2 The sum of two subspaces is defined as U V

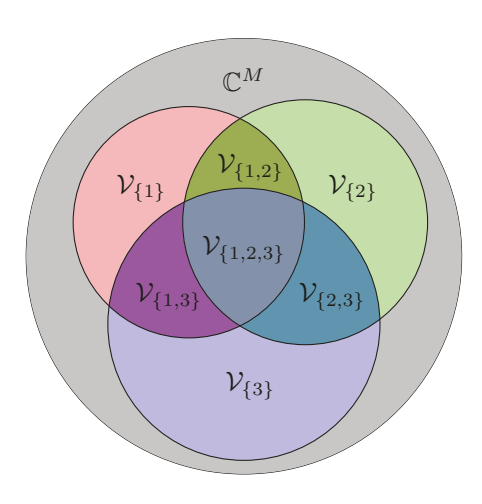


Fig. 6. The channel eigenspace overlapping structure of the three-user broadcast channel.

The interference graph G(K,k) has $\binom{K}{k}$ vertices. It is a regular graph [39, Sec. 1.2] of degree $\binom{K}{k} - \binom{K-k}{k} - 1$, with the convention $\binom{m}{n} = 0$ if m < n. Let $\chi(G(K,k))$ denote the chromatic number of G(K, k), i.e., the minimum number of colors to color all the vertices such that adjacent vertices have different colors. We have the following property.

Property 1 (The chromatic number of the interference graph). $\chi\big(G(K,1)\big) = 1, \ \chi\big(G(K,k)\big) \leq \binom{K}{k} - \binom{K-k}{k} - 1 \ \text{when} \ 1 < k \leq \lfloor K/2 \rfloor, \ \text{and} \ \chi\big(G(K,k)\big) = \binom{K}{k} \ \text{when} \ k > \lfloor K/2 \rfloor.$

Proof. $\chi(G(K,1)) = 1$ since G(K,1) is edgeless. $\chi(G(K,k)) = {K \choose k}$ when $k > \lfloor K/2 \rfloor$ because in this case, G(K, k) is complete. The results for the case $1 < k \le |K/2|$ follows from Brook's theorem [39, Thm. 5.2.4].

Remark 6. To avoid pilot interference, pilots in $V_{\mathcal{J}}$ and $\mathcal{V}_{\mathcal{K}}$ need to be orthogonal in time if $\mathcal{J} \cap \mathcal{K} \neq \emptyset$, i.e, \mathcal{J} and K are connected in the interference graph. Pilots in $V_{.T}$ and V_K can be transmitted simultaneously if $\mathcal{J} \cap \mathcal{K} = \emptyset$, i.e., \mathcal{J} and \mathcal{K} are not connected. Therefore, the problem of pilot alignment can be interpreted as interference graph coloring: pilots can be transmitted at the same time without interference in the subspaces corresponding to vertices with the same color. The minimum total amount of time for pilot transmission, normalized by the subspace dimension, is therefore the minimum number of colors, which is the chromatic number of the graph.

A. CSIR

In this section, we assume the users have perfect CSIR.

Theorem 8. For the K-user broadcast channel with CSIR, for any integers d_T satisfy

$$d_{\mathcal{J}} \le r_{\mathcal{J}}, \quad \forall \mathcal{J} \subset [K],$$
 (87)

$$\sum_{\mathcal{J} \subset [K]: \ k \in \mathcal{J}} d_{\mathcal{J}} \le \min(r_k, N_k), \quad \forall k \in [K], \quad (88)$$

the DoF tuple (d_1, \ldots, d_K) given by

$$d_k = \sum_{\mathcal{J} \subset [K]: \ k \in \mathcal{J}} \tau_{k,\mathcal{J}} d_{\mathcal{J}}, \quad k \in [K],$$
 (89)

for some time-sharing coefficients $\tau_{k,\mathcal{J}} \geq 0$ satisfying $\tau_{k,\mathcal{J}} =$ $0, \forall k \in \{[K] \setminus \mathcal{J}\} \text{ and } \sum_{i=1}^{K} \tau_{k,\mathcal{J}} = 1, \forall \mathcal{J} \subset [K], \text{ is}$ achievable.

Proof. For $\mathcal{J} \subset [K]$, let $\mathbf{V}_{\mathcal{J}} \in \mathbb{C}^{M \times d_{\mathcal{J}}}$ be a matrix with orthonormal columns such that $\mathrm{Span}\left(\mathbf{V}_{\mathcal{J}}\right)\subset\mathcal{V}_{\mathcal{J}}.$ Then $\mathbf{U}_{k}^{\mathsf{H}}\mathbf{V}_{\mathcal{J}}=\mathbf{0},\ \forall k\notin\mathcal{J},\ \mathrm{and}\ \mathrm{rank}\left(\mathbf{U}_{k}^{\mathsf{H}}\mathbf{V}_{\mathcal{J}}\right)=d_{\mathcal{J}},\ \forall k\in\mathcal{J}.$ Let the transmitter send the signal

$$\mathbf{X} = \sum_{\mathcal{J} \subset [K]} \mathbf{V}_{\mathcal{J}} \mathbf{s}_{\mathcal{J}},\tag{90}$$

where $\mathbf{s}_{\mathcal{J}} \in \mathbb{C}^{d_{\mathcal{J}}}$ contains data symbols. Let us consider User kand label the subsets in $\{\mathcal{J} \subset [K] : k \in \mathcal{J}\}$ as $\{\mathcal{J}_1, \dots, \mathcal{J}_l\}$. The received signal at User k is

$$\mathbf{Y}_{k} = \mathbf{G}_{k} \mathbf{\Sigma}_{k}^{\frac{1}{2}} \mathbf{U}_{k}^{\mathsf{H}} [\mathbf{V}_{\mathcal{J}_{1}} \dots \mathbf{V}_{\mathcal{J}_{l}}] \begin{bmatrix} \mathbf{s}_{\mathcal{J}_{1}} \\ \vdots \\ \mathbf{s}_{\mathcal{J}_{l}} \end{bmatrix} + \mathbf{W}_{k}. \tag{91}$$

Because $\sum_{i=1}^{l} d_{\mathcal{J}_i} \leq \min(r_k, N_k)$, User k can decode $\mathbf{s}_{\mathcal{J}_1}, \dots, \mathbf{s}_{\mathcal{J}_l}$, that is, $\{\mathbf{s}_{\mathcal{J}} \subset [K] : k \in \mathcal{J}\}$, where the signal $\mathbf{s}_{\mathcal{J}}$ provides $d_{\mathcal{J}}$ DoF. Signal $\mathbf{s}_{\mathcal{J}}$ can be decoded by all the users in \mathcal{J} . By dedicating $\mathbf{s}_{\mathcal{J}}$ to user $k \in \mathcal{J}$ in a fraction $\tau_{k,\mathcal{J}}$ of time, User k can achieve $\sum_{\mathcal{J} \in [K]: k \in \mathcal{J}} \tau_{k,\mathcal{J}} d_{\mathcal{J}}$ DoF. This completes the proof.

B. No Free CSIR

When the receivers have no free CSIR, we employ pilotbased schemes. As for the two-user case, we first consider the special case of fully overlapping eigenspaces and propose a product superposition scheme.

1) Fully Overlapping Eigenspaces:

Theorem 9. For the K-user broadcast channel without free CSIR and the correlation eigenvectors are nested such that $\mathbf{U}_{k-1} = [\bar{\mathbf{U}}_k \ \mathbf{U}_k]$ with $\bar{\mathbf{U}}_k$ being a basis of the complement of Span (\mathbf{U}_k) in Span (\mathbf{U}_{k-1}) , $k \in \{2, 3, \dots, K\}$, the DoF tuple (d_1, \ldots, d_K) given by

$$d_{1} = N_{1}^{*} \left(1 - \frac{r_{1}}{T} \right) \quad and$$

$$d_{k} = N_{k}^{*} \frac{r_{k-1} - r_{k}}{T}, \quad k \in \{2, 3, \dots, K\}$$
 (92)

is achievable.

Proof. We develop the idea in the special case of 3 users, and then proceed to describe the K-user result. When K=3, the transmitter sends

$$\mathbf{X} = \mathbf{U}_1 \mathbf{X}_2 \mathbf{X}_1, \tag{93}$$

$$\mathbf{X} = \mathbf{U}_{1} \mathbf{X}_{2} \mathbf{X}_{1}, \qquad (93)$$

$$\mathbf{m} \ \mathbf{8.} \ \textit{For the K-user broadcast channel with CSIR, for egers $d_{\mathcal{J}}$ satisfy} \qquad \text{with } \mathbf{X}_{1} = [\mathbf{I}_{r_{1}} \ \mathbf{S}_{1}] \in \mathbb{C}^{r_{1} \times T}, \ \mathbf{X}_{2} = \begin{bmatrix} \bar{\mathbf{X}}_{2} \\ \mathbf{X}_{3}[\mathbf{I}_{s_{2}} \ \mathbf{S}_{2}] \end{bmatrix} \in \mathbb{C}^{r_{2} \times r_{2}}, \text{ where } \bar{\mathbf{X}}_{k} \in \mathbb{C}^{r_{2} \times r_{2}}, \text{ where }$$

User , and contains symbols for User , . Because has orthogonal columns, the received signal at User is

(94)

User first estimates the equivalent channel and then decodes , achieving DoF.

The received signal at User during the first channel uses is

(95)

User estimates the equivalent channel in the first channel uses, then decodes in the next channel uses, achieving DoF.

The received signal at User during the first channel uses is

(96)

During the first channel uses, User estimates , and then during the next channel uses, User decodes its symbols, achieving DoF. Therefore, for , the normalized DoF tuple (92) is achieved.

Now, we apply the same idea to the case of users. The transmitted signal is

(97)

with

for , and

. User uses the same decoding method as the case of , achieving DoF. For users , consider the first channel uses, the received signal is

Therefore User can achieve — DoF. With the same decoding method as User in the case, User can achieve — DoF. This completes the proof of Theorem 9. \Box

2) Partially Overlapping Eigenspaces: We now consider the more general case of partially overlapping eigenspaces. We begin by analyzing symmetric -user channels with overlapped eigenspaces, offering an achievable DoF region with rate splitting. Subsequently, the asymmetric case will also be analyzed.

For symmetric channels:

$$\mathcal{J}$$
 \mathcal{J} \mathcal{J} \mathcal{J} \mathcal{J} (99)

That is, the rank of the common channel eigenspace $\mathcal{V}_{\mathcal{J}}$ is the same for all groups \mathcal{J} containing the same number of users. (In the two-user case, this corresponds to .) Define

$$\sigma$$
 T T (100)

for . Then the set of parameters characterizes the correlation structure of the -user symmetric broadcast channel. Furthermore, we assume that , . .

Theorem 10. The -user symmetric broadcast channel without free CSIR characterized by can achieve any permutation of the DoF tuple , for any , defined by

(101)

for , where

Let us first describe the achievable scheme in the 3-user case for clarity, then go for the -user case.

Example 1 (Achievable scheme for Theorem 10 for). When , the correlation structure is illustrated in Fig. 6. Under the symmetry assumption, we have , . The achievable scheme for

__ __ (102)

is based on rate splitting and channel training as illustrated in Table I.

Owing to linear precoding, choose a basis \mathcal{I} of the \mathcal{K} \mathcal{K} \mathcal{J} . It can be subspace spanned by ν \mathcal{J} . We choose the precoder proved that in this way but not directly choose a basis from \mathcal{I} , because for different \mathcal{J} , \mathcal{J} is not guaranteed to be *orthogonal* with each other and we aim to remove the interference from the other channel component in $\ _{\mathcal{K}}\ \mathcal{K}$ $\ \mathcal{J}$, so that all users in \mathcal{J} can learn the channel directions in $\mathcal{V}_{\mathcal{I}}$. From Remark 6, the required amount of pilot transmissions is identical with the chromatic number of the interference graph. The interference graph has chromatic number , which is also the amount of time, normalized by , needed for pilot transmission without interference in \mathcal{V} , \mathcal{V} , and \mathcal{V} . Similarly, it takes channel uses to transmit pilot interference-free in \mathcal{V} $, \mathcal{V}$, and \mathcal{V} , and takes channel uses for pilot transmission in \mathcal{V}

In this way, the total time for channel training is channel uses and there remains channel uses for simultaneous data transmission in all subspaces. By dedicating the data transmitted in $\mathcal V$, and $\mathcal V$ to User, User achieves — DoF. By dedicating the data transmitted in $\mathcal V$ to User, User achieves — DoF. User achieves — DoF from the data transmitted in $\mathcal V$. On top of that, the base station can transmit additional data to User in $\mathcal V$ by superimposing it with the pilot for User

 $\label{thm:table I} \textbf{TABLE I}$ Illustration of pilot and data alignment for the scheme achieving

\overline{v}	Pilot		Data			Data
\mathcal{V}	Pilot			Data		Data
\mathcal{V}	Pilot	Data				Data
\mathcal{V}		Pilot				Data
\overline{v}			Pilot			Data
$\overline{\mathcal{V}}$				Pilot		Data
\mathcal{V}					Pilot	Data

TABLE II ILLUSTRATION OF PILOT AND DATA ALIGNMENT FOR THE SCHEME ACHIEVING

\overline{v}	Pilot		Data		Data
\mathcal{V}	Pilot			Data	Data
\mathcal{V}	Pilot	Data			Data
\overline{v}		Pilot			Data
\overline{v}			Pilot		Data
\overline{v}				Pilot	Data
\mathcal{V}					

TABLE III
ILLUSTRATION OF PILOT AND DATA ALIGNMENT FOR THE SCHEME ACHIEVING

\overline{v}	Pilot	Data
\overline{v}	Pilot	Data
\overline{v}	Pilot	Data
$\overline{\nu}$		
\overline{v}		
\overline{v}		
\overline{v}		

vable scheme	t show the achievable	We first s	Proof of Theorem 10.	r and	Similarly, User	without interference.	ser in \mathcal{V}	and Us
	y	given by	for	ditional	With these addi	eceive additional data. Y	can also r	User
					fore,	chieves — DoF. There	ach user ac	data, e
							ieved.	is achi
			_			, which is	achieve	To a
(10.1)								
(104)								
	P44'		TTL 1					
training with	nuing and channel trail	n rate spiitt	The scheme is based of	(103)				

we simply ignore the subspace $\mathcal V$. Then, we do not send pilot in this subspace and have more time to send data in all other subspaces. As a price for that, we lose the data we could send in $\mathcal V$ during the last channel uses. When $\mathcal V$ is small enough, this loss is not significant and we can gain DoF. The achievable scheme is illustrated in Table II.

Illustrated in Table II.

Similarly,

— can be achieved by ignoring \mathcal{V} , \mathcal{V} \mathcal{V} , and \mathcal{V} , as illustrated in Table III.

Due to symmetry, any permutation of, is achieved by permuting the users' indices.

The scheme is based on rate splitting and channel training with two key elements: alignment of pilots in different subspaces, and superposition of additional data on top of pilots without causing interference.

User needs to learn the channel directions in all subspaces $\mathcal{V}_{\mathcal{J}}$ such that \mathcal{J} and is oblivious to signals (pilot or data) transmitted in other subspaces. From Remark 6, the minimum total amount of time for pilot transmission in the common subspace by k users, normalized by the subspace dimension is given by the chromatic number of the interference graph . Thus the total training time is channel uses. In the remaining channel uses, data is transmitted in all subspaces. The DoF that User , \mathcal{J} , can achieve with the message transmitted in $\mathcal{V}_{\mathcal{J}}$ is - $\mathcal{V}_{\mathcal{J}}$

Notice that for any $l > \lfloor K/2 \rfloor$, the interference graph G(K,l) is fully connected, the pilots in subspaces $\mathcal{V}_{\mathcal{K}}$ for $|\mathcal{K}| = l$ cannot be transmitted at the same time. However, additional data can be transmitted in any subspace $\mathcal{V}_{\mathcal{J}}$ such that $\mathcal{V}_{\mathcal{K}} \cap \mathcal{V}_{\mathcal{J}} = \emptyset$. In this way, during the training of all subspaces $\mathcal{V}_{\mathcal{K}}$ with $|\mathcal{K}| = l$, for each subset \mathcal{J} which does not intersect with $|\mathcal{K}|$, additional data can be transmitted in $\binom{K-|\mathcal{J}|}{l}p_l$ channel uses, enabling each user in \mathcal{J} to achieve $\frac{1}{T}\binom{K-|\mathcal{J}|}{l}p_{\mathcal{J}}p_l$ more DoF.

Summing up the DoF, the number of DoF that each user in \mathcal{J} can obtain from the message transmitted in $\mathcal{V}_{\mathcal{I}}$ is

$$\frac{1}{T}p_{|\mathcal{J}|}\left(T - T_{\tau}(K, 0)\right) + \frac{1}{T} \sum_{l=\lfloor K/2 \rfloor+1}^{K} {K - |\mathcal{J}| \choose l} p_{|\mathcal{J}|} p_{l}$$

$$= \frac{1}{T}p_{|\mathcal{J}|}\left(T - T_{\tau}(K, 0) + \sum_{l=\lfloor K/2 \rfloor+1}^{K} {K - |\mathcal{J}| \choose l} p_{l}\right). (105)$$

By dedicating all the messages transmitted in $\mathcal{V}_{\mathcal{K}}$ such that $k \in \mathcal{J}$ and $\mathcal{J} \cap [k-1] = \emptyset$ to User k, User k achieves d_k DoF where d_k is given in (104). Then $D_{K,0}(p_1,\ldots,p_K)$ is achievable.

Similar to the 3-user case, $D_{K,L}(p_1,\ldots,p_K)$ with $L\in [K-1]$ is achieved by ignoring all the subspaces $\mathcal{V}_{\mathcal{J}}$ with $|\mathcal{J}|>K-L$. Finally, due to symmetry, any permutation of $D_{K,L}(p_1,\ldots,p_K)$ with $L=1,\ldots,K-1$ can be achieved by permutting the users' indices. \square

Remark 7. We can improve the achievable scheme by sending additional data during the training of V_K with $|K| \leq \lfloor K/2 \rfloor$ also. However, the possibility for this additional data depends on the actual coloring of the interference graph and would not admit nice expressions of achievable DoF tuples. We therefore do not follow this direction in the interest of developing closed-form expressions.

Computing the chromatic number $\chi(G(K,k))$ is NP-complete in general [40]. Therefore, one might confine to the achievable DoF tuples in the following corollary.

Corollary 4. The K-user symmetric broadcast channel without free CSIR can achieve the DoF tuple $D_{K,l}(p_1,\ldots,p_K)$ given in Theorem 10, with $T_{\tau}(K,L)$ replaced by $\sum_{k=1}^{K-L} {K \choose k} - {K-k \choose k} - 1\{1 < k \leq \lfloor K/2 \rfloor\} p_k$.

This corollary follows from Theorem 10 and Property 1. Based on Theorem 10, we have the following achievable DoF region for the symmetric K-user channel.

Theorem 11. The K-user symmetric MIMO broadcast channel without free CSIR characterized by (p_1, \ldots, p_K) can achieve the convex hull of all permutations of any DoF tuple of the form

$$(D_{k,L}(p_1^*,\ldots,p_k^*),0,\ldots,0), k \in [K], L \in \{0,\ldots,k-1\},$$

with $D_{k,L}(\cdot)$ defined according to (101) and $p_l^* = \sum_{i=0}^{K-k} {K-k \choose i} p_{l+i}$ for $l \in [k]$.

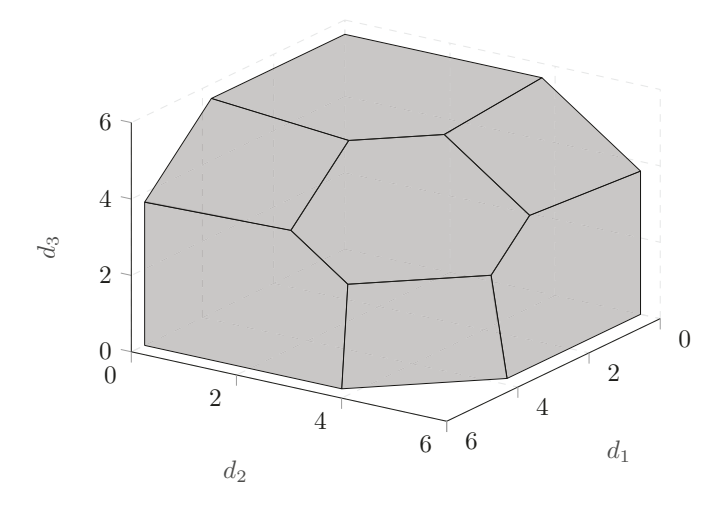


Fig. 7. An achievable DoF region of the symmetric 3-user non-coherent broadcast channel with spatial correlation with $T=24, r_{\{1\}}=r_{\{2\}}=r_{\{3\}}\triangleq p_1=4, r_{\{1,2\}}=r_{\{1,3\}}=r_{\{2,3\}}\triangleq p_2=2,$ and $r_{\{1,2,3\}}\triangleq p_3=1.$

Proof. When k = K, (106) becomes $D_{K,L}(p_1, \ldots, p_K)$, which can be achieved as stated in Theorem 10.

When k < K, by ignoring the last K-k users, we construct a new symmetric channel with k users. For example, by ignoring User 3 in the symmetric 3-user channel, we obtain a two-user channel in which the private subspace of User 1 and User 2 are $\mathcal{V}_{\{1\}} + \mathcal{V}_{\{1,3\}}$ and $\mathcal{V}_{\{2\}} + \mathcal{V}_{\{2,3\}}$, respectively, both of dimension $p_1^* = p_1 + p_2$; whereas the common subspace of two users is $\mathcal{V}_{\{1,2\}} + \mathcal{V}_{\{1,2,3\}}$ of dimension $p_2^* = p_2 + p_3$. In general, the new K-user channel is characterized by the new set of parameters (p_1^*, \ldots, p_k^*) , where $p_l^* = \sum_{i=0}^{K-k} {K-k \choose i} p_{l+i}$, $l \in [k]$. Then, applying Theorem 10 to this k-user symmetric channel, the rate region $D_{k,L}(p_1^*, \ldots, p_k^*)$ is achievable. Therefore, $(D_{k,L}(p_1', \ldots, p_k'), 0, \ldots, 0)$ is achievable for the original K-user symmetric channel. Any permutation of (106) can be achieved by permuting the users' indices.

Fig. 7 demonstrates the achievable DoF region for the symmetric 3-user broadcast channel given in Theorem 11 with $T=24, r_{\{1\}}=r_{\{2\}}=r_{\{3\}}=4, r_{\{1,2\}}=r_{\{1,3\}}=r_{\{2,3\}}=2,$ and $r_{\{1,2,3\}}=1.$

We now broaden our analysis to K-user channels that may be *asymmetric*. The achievable scheme combines product superposition and rate splitting.

Theorem 12. The K-user broadcast channel without free CSIR can achieve the DoF tuple (d_1, \ldots, d_K) given by

$$d_k = \sum_{\mathcal{J} \subset [k]: \ k \in \mathcal{J}} r_{\mathcal{J}} \left(1 - \frac{r_k}{T} \right)$$

$$+ \sum_{l=k+1}^K \sum_{\mathcal{J} \subset [K]: \ k \in \mathcal{J}, |\{k+1,\dots,K\} \cap \mathcal{J}| < 2} r_{\mathcal{J}} \frac{r_l - r_k}{T}, \quad (107)$$

where it is assumed without loss of generality that $r_K \ge r_{K-1} \ge \cdots \ge r_1$.

Proof. For simplicity, let us focus on the 3-user case. We assume without loss of generality that $r_3 \geq r_2 \geq r_1$. For each partition $\mathcal{V}_{\mathcal{J}}$, $\mathcal{J} \subset [3]$, we build a precoder $\mathbf{V}_{\mathcal{J}} \in \mathbb{C}^{M \times r_{\mathcal{J}}}$ as

(110)

(113)

and

. User

an orthonormal basis of $\mathcal{V}_{\mathcal{J}}$, thus $^{\mathsf{H}}_{\mathcal{J}}$, \mathcal{J} , and $^{\mathsf{H}}_{\mathcal{J}}_{\mathcal{J}}$, \mathcal{J} . To combine rate splitting and product superposition, the transmitted signal is

(108) (118)

with

where ,

(109)

learns the equivalent channel **H**in the first channel uses then decode , and to achieve —— —— —— —— —— DoF in total.

(111) Therefore, the 3-user broadcast channel can achieve the DoF triple

(119)

where and are designed to guarantee that and are respectively non-singular.

The received signal at User is

H

User estimates the equivalent channel
H in the first channel
uses and then decode to achieve full individual DoF

The received signal at User is

H (115)

(116)

where . User can learn the equivalent channel ${\bf H}$ in the first channel uses and then decode both and to achieve — DoF in total.

The received signal at User is

Н

H
H
(117)

Using similar reasoning, for the general -user case such that , the DoF in (107) is achievable.

VII. APPLICATION IN MASSIVE MIMO

In a massive MIMO system [41], the base station needs the CSI to beamform. However, due to the large number of antennas, the overhead for channel estimation is large. On the other hand, due to the limited space between the transmit antennas, the channel responses are normally spatially correlated. In this section, we exploit the spatial correlation to reduce the training overhead and compare the scheme with conventional training method.

We consider a multi-user massive MIMO system with a base station equipped with antennas communicating with single-antenna users with different spatial correlations. The channel vector corresponding to user is ... The received signal of User at time is The received signal of user at time is and during a coherence block is

т т (120)

where and $^{\rm T}$ \mathcal{CN} . We assume that the system operates in FDD mode and focus on the downlink transmission. The transmission has two phases: the pilot phase and the data phase. During the pilot phase, pilot signal is sent so that the users can estimate the channel and then feedback the channel estimates to the base station. For simplicity and to focus on the gain of exploiting spatial correlation, we asume that feedback is perfect and instantaneous. After that, the base station sends data via beamforming.

A. The Two-User Case

We first consider the two-user scenario and assume that User has uncorrelated channel and User has spatially correlated channel of rank . To extract an uncorrelated equivalent representation of , we define via

$$\mathbf{U}$$
 (121)

where $^{\mathsf{T}}$ is a truncated unitary matrix.

Consider one coherence block. During the pilot phase, the transmitted signal is

where for , and is a Gaussian random variable following \mathcal{CN} for , the received signal at User is T User estimates with a MMSE estimator

The estimation error is In time slots , User receives the signal User uses the estimated channel to decode , achieving the rate

The received signal at User in the pilot phase is

User estimates $^{\mathsf{T}}$ by $^{\mathsf{T}}$ and feeds back to the base station. Because the base station knows obtain the estimation of as $^{\mathsf{T}}$ The estimation error is

Let and . During the data phase, i.e. time slots , the transmitted signal via conjugate beamforming is $-\frac{h}{h} \qquad -\frac{h}{h}$ where is the data symbol for user following the \mathcal{CN} distribution. The received signals at the two users are

The achievable rate for User is:

$$-$$
 (128)

where the equivalent SNRs are defined as $\frac{\mathbf{h}^T\mathbf{h}}{\mathbf{h}} = \frac{\mathbf{h}^T\mathbf{h}}{\mathbf{h}} = - \quad \text{and}$ $\frac{\mathbf{h}^T\mathbf{h}}{\mathbf{h}} = \frac{\mathbf{h}^T\mathbf{h}}{\mathbf{h}} = - \quad \text{The achievable sum rate}$ is

For conventional transmission, the transmitter ignores the condition that two users need different number of pilots and sends pilots over time slots, the users estimate the channel and feedback to the transmitter. Then the transmitter communicates with the users via conjugate beamforming [41]. Figure 8 shows the performance of the proposed scheme in comparison with the conventional one under Rayleigh fading, , , User has fully correlated channel and User has uncorrelated channel.

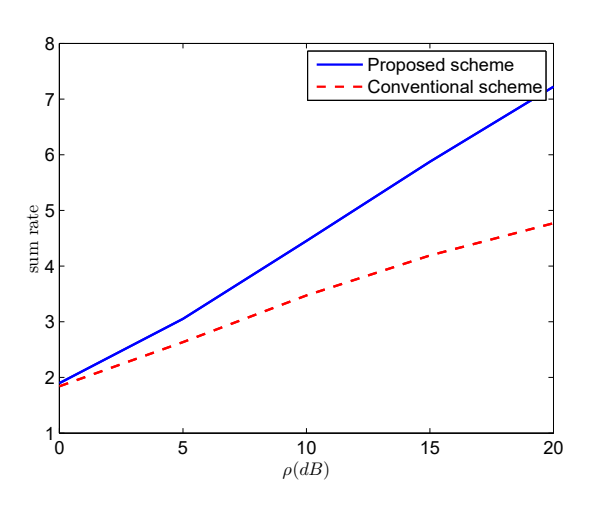


Fig. 8. The sum rate of the considered FDD massive MIMO system with the proposed scheme in comparison with the conventional scheme for , , User has fully correlated channel, and User has uncorrelated channel.

We now generalize to the case where both users experience spatially correlated links and have partially overlapping eigenspaces. Recall that the eigendirections for the two users are , where , for . We assume without loss of generality that . We find transmit eigendirections with orthonormal columns that are aligned with the common part of the two channel eigenspaces and that are aligned with the non-common parts, i.e.,

\ (1)

Therefore, we can write where ,

The proposed scheme has two phases. The pilot phase has time slots, and the data phase has time slots. In the pilot phase, the base station sends pilots in the subspace of in time slots 1 to , The received signal at User is

that

(136)

In the next time slots, the base station sends pilots to two users simultaneously in subspaces and , the transmitted signal is

The received signals at two users are:

Based on T , User obtains a MMSE estimates

of and feeds back to the base station. The estimation error is . In time slots to , the base station sends pilots for User in the remaining eigenspaces and sends data to User via beamforming as

where contains i.i.d. \mathcal{CN} data symbols. The received signal at User is:

Based on T , User obtains a MMSE estimates

of and feeds back to the base station. The estimation error is

The received signal at User is

User decodes and achieves the rate

$$\frac{-}{-}\frac{\mathbf{g}^{\mathsf{T}}}{\mathbf{g}^{\mathsf{T}}}$$
 (142)

With the help of the feedback, the base station generates estimation for the two channels via , and The estimation errors are and . During the data phase, the transmitted signal via conjugate beamforming is

$$^{\mathsf{T}}$$
 $^{\mathsf{T}}$ (143)

where , contains i.i.d. \mathcal{CN} data symbols for User . The received signals at the two users are

User decodes and achieves the rate

with the equivalent SNRs $\frac{\mathbf{h}^{\mathsf{T}}\mathbf{h}}{\mathbf{h}} = \frac{\mathbf{h}^{\mathsf{T}}\mathbf{h}}{\mathbf{h}} = -$ and $\frac{\mathbf{h}^{\mathsf{T}}\mathbf{h}}{\mathbf{h}} = \frac{\mathbf{h}^{\mathsf{T}}\mathbf{h}}{\mathbf{h}} = -$. The achievable sum rate is:

In the next subsections, we consider the —user case. In this case, for a general (irregular) correlation structure, the signal design matching the correlations is complicated. Therefore, in order to emphasize the gain of correlation-based rate splitting and product superposition, we focus on some special configurations of the eigenspaces.

B. The -User Case with Symmetric Eigenspace

The first considered special eigenspace configuration for the -user case is the symmetric correlation structure as in VI-B2. We first present the case when . Under the symmetry assumption, we have . ,

, and .

Define the matrix as the collection of all the eigendirection vectors, which means

where $_{\mathcal{J}}$ $^{\mathcal{J}}$ contains the eigenvectors spanning the subspaces of all users in \mathcal{J} . Now we decompose the channel as $_{\mathcal{J}}$ $_{\mathcal{J}}$ where . For example,

In the first time slots, the base station sends pilots to three users simultaneously in subspaces , and . The transmitted signal is

The received signal at User is

$$\stackrel{\mathsf{T}}{}$$
 $\stackrel{\mathsf{T}}{}$ $\stackrel{\mathsf{T}}{}$ (150)

User estimates $^{\mathsf{T}}$ to obtain $^{\mathsf{T}}$ and feeds back to the base station. The estimation error is $^{\mathsf{T}}$

To the next time slots, the base station sends pilots to users and in the subspace of and data to the remaining user via conjugate beamforming. For example, in the first time slots, it sends

where contains i.i.d. \mathcal{CN} data symbols. The received signal at User or User is

User estimates
$$^{\mathsf{T}}$$
 to obtain $^{\mathsf{T}}$ and feeds back to the base station. The received signal at User is

User decodes and achieves the rate

$$-\frac{\frac{-}{\mathbf{h}^{\mathsf{T}}\mathbf{V} \quad \mathbf{V}^{\mathsf{T}} \quad \mathbf{h}}{\mathbf{V}^{\mathsf{T}} \quad \mathbf{h}}$$
(155)

In the subsequent time slots, the channel coefficients in $\mathcal V$, $\mathcal V$ are estimated and and fed back, and the achievable rate for User and User can be calculated similarly.

In the following time slots, the base station transmits pilots in ${\cal V}$ as — User receives — $^{-}$ $^{\rm T}$. es-

timates ^T to obtain ^T and feeds back to the base station. From the feedbacks in the first time slots the base station obtains estimates of

time slots, the base station obtains estimates of . The estimation error is .

During the data phase, the transmitted signal via conjugate beamforming is

where contains i.i.d. \mathcal{CN} data symbols for User . The received signals at User is

User decodes and achieves the rate,

The achievable rate of User and User can be calculated in the same way.

The achievable sum rate is

Now we extend this scheme to the -user scenario. Following the signaling structure developed in the -user case, the transmit scheme has three phases. In the first phase, some pilot signals are transmitted. In the second phase, the remaining pilots are transmitted while at the same time, some users also receive data. In the third phase, channel state is known (due to pilots transmitted in the earlier two phases) and the base station beamforms to all users. The pilots and data arrangement is similar to the achievable scheme for Theorem 10.

The first phase has time slots, in the first time slots, the base station sends — . In the same way, during the following time slots, the base station sends pilots which will not interfere with each other. The users estimate the channel coefficients in these subspaces and feed back to the base station.

The second phase has time slots, where . In this phase, the base station sends pilot in some eigendirections and simultaneously beamforms to the users which are not interfered by the pilots. For example, when sending the pilots in $\mathcal V$, the transmitted signal is

where the equivalent channels ^T and ^T have been estimated and fed back in the first phase. During these time slots, User to User can estimate their channel coefficients in the direction of user can decode and User can decode .

In the third phase, which has time slots, the base station beamforms to all users with the estimated channel by sending

at time slot .

Finally, the total rate that can be achieved is the sum of the rates achieved during phases two and three.

C. The -User Case with On-Off Correlation

The second special correlation configuration is motivated as follows. Experience shows that small values of correlation are often inconsequential to the rate and thus can be treated as uncorrelation in signal design. Furthermore, interferencefree pilot reuse is only made possible under rank deficient correlation matrices, i.e., some transmit antenna gains are fully deterministic conditioned on the others. Therefore, we consider -user channel where the pairs of transmit antennas are either uncorrelated or fully correlated for each user, and refer to it as on-off correlation. Specifically, consider the channel ^T of any User , for any vector , we assume that either (fully correlated) or (uncorrelated).

The base station transmits the following signal in the pilot phase:

where and , — , (162) are mutually independent random variables following the

are mutually independent random variables following the distribution \mathcal{CN} . Here are the symbols for User and is for one of the users in group . The received signal at User is:

$${}^{\mathsf{T}} \qquad {}^{\mathsf{T}} \mathbf{X} \qquad {}^{\mathsf{T}} \tag{163}$$

User estimates \mathbf{X}^{T} via MMSE and feeds back the estimated version — to the base station. Because the base station knows \mathbf{X} , it obtains an estimated version of the channel of User as — \mathbf{X}^{T} . The estimation error is

Denote the fully correlated channel coefficient of User . In the first time slot, as User . It estimates receives and the estimation error is $\mathcal{C}\mathcal{N}$ We have that $\mathcal{C}\mathcal{N}$ and . In , User the time slots receive . User can decode and achieves the rate

— (164)

— (165)

```
(166)
where
                          is the exponential integral function.
                          is assigned to group
  In addition, if User
        , denote
                             . In time slot -
                                                        , the
received signal of User is
                                                       (167)
      can estimate the equivalent channel
User
                     and the estimation error is
                . We have that
                                                        and
                  In the next —
                                           time slots, User
receives
                                                       (168)
                         . Therefore, User
and achieve the rate
                                                       (169)
```

In the beamforming phase, the base station beamforms to the users according to the estimated channel with equal power. The transmitted signal is

where contains i.i.d. \mathcal{CN} data symbols for User . The received signal at User is:

User decodes and achieves the rate

$$\frac{-\frac{\mathbf{h}^{\mathsf{T}}\mathbf{h}}{-\frac{\mathbf{h}^{\mathsf{T}}\mathbf{h}}{\mathbf{h}}} \frac{\mathbf{h}^{\mathsf{T}}\mathbf{h}}{\mathbf{h}}$$
(174)

Finally, the achievable sum rate is:

(175)

(170)

Figure 9 shows the performance gain of the proposed scheme with respect to the conventional one under the following configuration: , , , . . .

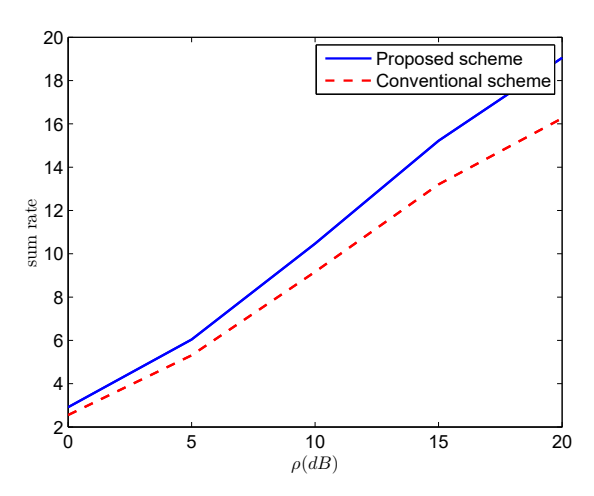


Fig. 9. The sum rate of the considered FDD massive MIMO system in on-off correlated fading with the proposed scheme in comparison with the conventional scheme for

D. Discussion: Correlation Diversity in Massive MIMO

Our work focuses on gains that can be gleaned from the allocation of pilots. Broadly, our work has gains when the spatial correlation matrices between the users are dis-similar. The more the dissimilarity of the correlation matrices, the higher the gains provided by our technique. The metric for similarity in our work is the alignment of the null spaces of the transmit correlation matrices corresponding to different users. A more detailed analysis of the gains depends naturally on antenna numbers as well as other factors; we omit a detailed listing of these cases in the interest of brevity.

In massive MIMO, when receivers have non-identical transmit correlations, designing the training sequences to match these non-identical channel correlation matrices can be challenging. Under this condition, Jiang et al. [42] propose a scheme for massive MIMO in which the pilots are optimized according to a mutual information metric, and optimal length of the pilots is found by exhaustive search. When users have correlation matrices with different ranks, our method will have significant gains (in multiplexing gain) over [42].

VIII. DISCUSSION AND CONCLUSION

This paper extends the scope of transmit correlation diversity to a broader set of conditions involving transmit correlation matrices with fully and partially overlapping eigenspaces. Furthermore, we present transmission schemes that harvest these generalized correlation diversity gains. We demonstrate the utility of both pre-beamforming and product superposition for correlation diversity. This arises from a careful decomposition of transmission spaces into several components. Along non-overlapping eigenspaces, simultaneous and non-interfering transmission is possible, as noted by earlier work. In the overlapping part, one may utilize the techniques employed in this paper. Careful design of this decomposition is necessary to allow the effective carving of the transmission signal space, allowing efficient operation of the proposed techniques. These ideas were developed in the context of a two-user system and

were extended to multi-user systems. The application of these ideas in a massive MIMO system was explored.

In the interest of completeness, we mention imperfect or partial CSIT [43], [44] as another situation in which the transmitter knows something about the channel, but not everything. In transmit correlation diversity, training is concentrated on the part of the channel that remains unknown, while the imperfect/partial CSIT literature investigates how much of the channel knowledge can be abandoned in the interest of feedback efficiency, and what is the cost of this abandonment. In that sense, the two areas of investigation might be considered the dual of each other. Partial CSIT varies from one channel realization to the next, and is subject to fading speed and efficiency of feedback, while transmit correlation diversity reflects longer-term statistics that can be collected in the receiver over many realizations, and due to its slower variation, can be communicated with transmitter at higher precision. The methods and techniques used in addressing correlation diversity in this paper are largely distinct from the literature of imperfect/partial CSIT.

IX. ACKNOWLEDGEMENT

The authors gratefully acknowledge Dr. Maxime Guillaud for his contribution to this investigation.

APPENDIX A PROOF OF THEOREM 4

We prove by constructing pilot-based schemes that can achieve (49), (50), and (51).

A. Case 1: Transmitter Ignores Correlation

The transmitter can ignore and form the transmitted signal as if the channel is uncorrelated, but the performance still depends on correlation. Within each coherence block, the transmitter first sends an orthogonal pilot matrix

such that $^{\rm H}$ during the first channel uses (this is optimal for uncorrelated fading [24, Sec. III-A]), and then sends i.i.d. \mathcal{CN} data matrix during the remaining channel uses. That is,

(178)

where and are the average power used for training and data phases, respectively, and satisfy the power constraint

In the training phase, the receiver observes

_____ . Following Lemma 3, it performs a linear MMSE channel estimator as

The estimate and the estimation error have zero mean and row covariance

— н (179)	The estimate and the estimation error have zero mean and row covariance
In the data transmission phase, the received signal is	— ^н — — ^н (190)
<u>—</u> —	· ,
_	_ н н
(180)	— н (191)
where — is the combined noise consisting of additive noise and channel estimation error. With MMSE estimator, and are uncorrelated because	In the data transmission phase, the received signal is
н н н н	
(181)	
H (182)	where — . From Lemma 2, a lower bound on the achievable rate is obtained by replacing with i.i.d. Gaussian noise with the same variance
(183)	н
since . From Lemma 2, a lower bound	w ———
on the achievable rate is obtained by replacing by i.i.d. Gaussian noise with the same variance	— — H (193)
	The corresponding achievable rate lower bound is
W (104)	——————————————————————————————————————
(185)	where the rows of O obey CN with
	— H and are independent with each other.
Thus, the achievable rate is lower bounded by	Taking such that H (i.e., orthogonal pilots) we have , and the achievable rate is
$$ W (187)	given in (50). We can also optimize the pilot so as to maximize
From (178), has correlation matrix . This shows (49).	The pilot matrix affects the achievable rate bound primarily through the effective SNR
	— н (195)
B. Case 2: Transmitter Exploits Correlation	which decreases with . Therefore, to maximize , we
By exploiting the transmitter can project the signal onto and can also adapt the pilot symbols. The transmitter builds a precoder with orthonormal	would like to minimize . That is
columns such that . Let H . The	$\mathbf{X}^{H}\mathbf{X} \tag{196}$
transmitted signal is	Using Lagrange multiplier , we minimize
<u> </u>	н н
where such that and H	(197)
where such that and is the pilot matrix, and is the data matrix containing \mathcal{CN} entries. The average pilot and data powers satisfy	Solving $\frac{\mathbf{X}}{\mathbf{X}\mathbf{X}^{H}}$, we obtain the minimizer \mathbf{X} . Using the constrain \mathbf{X} , we
The received signal during the training phase is then	find that — H — With this.
The equivalent channel	- , and the rate is given in (51)
has correlation matrix H H . According to Lemma 3, the MMSE channel estimate for the equivalent channel is given by	The effective SNR is now written as
H (189)	- - (198)

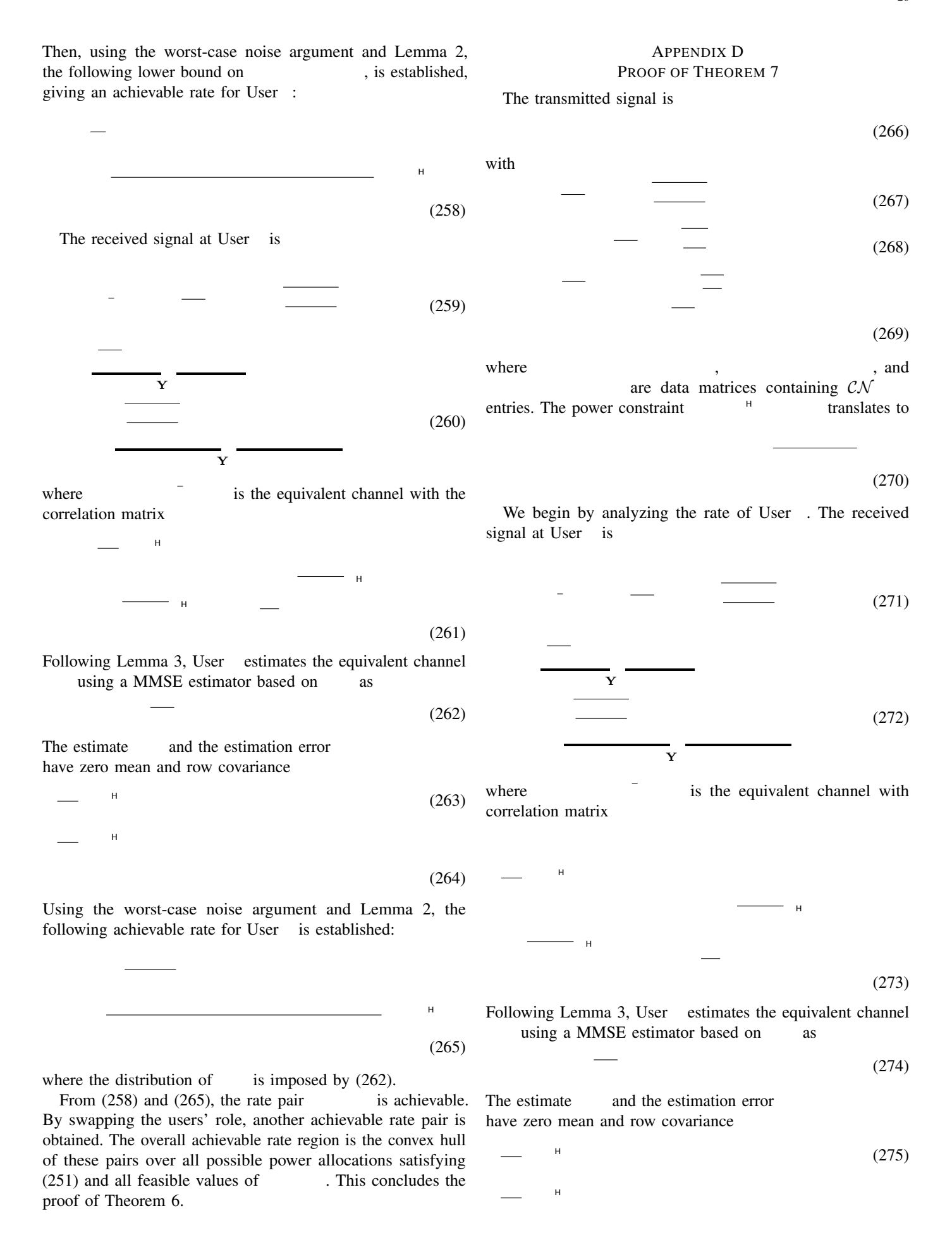
Remark 2 follows from an optimization of () as follows Let and for we can derive that	The estimate and the estimation error have zero mean and row covariance
we can derive that	н
(199)	(207)
where $\frac{R}{R}$ and $\frac{R}{R}$ and $\frac{R}{R}$ Noting that , we obtain the optimal value of that	н
maximizes as given in (52). This completes the proof.	
APPENDIX B PROOF OF THEOREM 5	(208)
This achievable rate region is fully characterized by the mutual information , , and	the data transmission phase can be written as
, . We cacluate the achievable rates for the following input distribution:	(209)
(200)	where is the combined
<u> </u>	noise and residual interference due to channel estimation error. Define with independent rows
(202)	similar analysis using Lemma 2 as for (50) in Theorem 4,
where , , and are data matrices containing independent	
\mathcal{CN} symbols, for powers , , such that	(210)
(203)	(211)
The received signal at User is	н (212)
- — <u> </u>	——————————————————————————————————————
(204)	н н
	(213)
Y	Lower bounding : We rewrite as
(205)	
Y	(214)
where and	While decoding , the term — is an interference. Given the knowledge of and the channel estimate
are the power matrices for the pilot	
and data, respectively.	partly the interference to obtain
The equivalent channel has correlation matrix . Following Lemma 3, User channel estimation based on as	
(206)	

(215)	
(216)	Y
With a similar analysis using Lemma 2 as for (50) in Theorem 4,	
Theorem 1,	(230)
(217)	
(218)	Y
	where and are respectively the first columns and the remaining columns of ;
	and are the
(220)	power matrices for the pilot and data, respectively. Following Lemma 3, user 2 performs a MMSE channel estimation of
н н	based on as
(221)	(231)
Lower bounding : Given and the channel	The estimate and the estimation error
estimate , the receiver can remove partly	have zero mean and row covariance
the interference in (214) to obtain	н
<u> </u>	(232)
	н
(222)	
(223)	(233)
Using reasoning similar to (50) in Theorem 4,	Lower bounding : Using the chain rule,
	Lower boundaring . Coming the chain rule,
(224)	(234)
(225)	,
— (226)	(235)
(227)	(236)
н н	
(228)	$\mathbf{Y} \mathbf{S} \mathbf{S} \mathbf{\Omega}$ (237)
The received signal at User is	
	(238)
_ =	Define with independent rows obeying
	\mathcal{CN} . Following analysis similar to (50) in Theorem 4,
(229)	

(257)

APPENDIX C PROOF OF THEOREM 6 (239)Under product superposition, the input to the channel is constructed as follows: and (248)with (249)(250)(240)Lower bounding : For where and are the we write it as data matrices of User and User respectively, both contain i.i.d. \mathcal{CN} symbols. As in earlier developments, integers are designed to allocate transmit dimensions to the components of product superposition, and take values in the (241)range and The power constraint translates to Similar to , using interference cancellation and wort-case additive noise, (251)(242)In the first channel uses, User (243)(252)Н (253)(244)Following Lemma 3, User estimates the equivalent channel Lower bounding : Again, using interference using a MMSE estimator based on as cancellation and a similar analysis as for (50) in Theorem 4, (254)(245)The estimate and the estimation error (246)have zero mean and row covariance (255)(247)(256)Substituting (239) and (240) into (238), then substituting (213), (221), (228), (238), (244), and (247) into (65)-(67), and Using data processing inequality, taking the convex hull over all possible power allocation satisfying (203) and all feasible values of , an achievable rate region is found with rate splitting for the broadcast channel.

This concludes the proof of Theorem 5.



	(276)	
Using the worst-case noise argument and Lemma 2 the following achievable rate for User is obtained		(286
		where and
	н	
		<u> </u>
where the distribution of is imposed by (274). Now, we turn to analyzing the achievable rate f The received signal at User can be written as	(277) or User .	The term can be upper bounded at follows:
	<u> </u>	
<u> </u>	_	(288
		(289
	(278)	(290
	(279)	(2)0
where — — and		- (291 -
	(280)	-
	(200)	(292
		(293
_	(201)	
	(281)	(204
- <u>-</u>		(294
	(282)	- (295
	()	
where . The rate that U	Jser can	н
achieve is - bits/channel use with		(296
	(283)	where (287) and (288) follow from the Markov chains
		and , respectively
	(20.4)	(289) holds because mutual information is non-negative and both and are independent of ; (291) holds
	(284)	both and are independent of ; (291) holds because conditioning reduces entropy; (292) holds because
	(285)	is independent of both and , while given
hander and a later and the Com-		depends on only through ; and in the las
where the second and third equalities follow from rule.	tne chain	equality, we used that — .
Define with independ	ent rows	Substituting (286) and (296) into (285), an achievable rate fo User is obtained. This rate and (277) give an achievable rate
obeying \mathcal{CN} ^H and	Г	pair. Taking the convex hull of this pair over all possible power
with independent rows obeying \mathcal{CN} , using the worst-case noise and Lemma 2 as before, we have the bound	. For argument	allocations satisfying (270) and all feasible values of provides an overall achievable rate region. This concludes the proof of Theorem 7.
		Decedences
н		REFERENCES
-		[1] J. P. Kermoal, L. Schumacher, K. I. Pedersen, P. E. Mogensen, and F. Frederiksen, "A stochastic MIMO radio channel model with experimental validation," <i>IEEE J. Sel. Areas Commun.</i> , vol. 20, no. 6, pp. 1211–1226, Aug. 2002.

- [2] K. Yu, M. Bengtsson, B. Ottersten, D. McNamara, P. Karlsson, and M. Beach, "Modeling of wide-band MIMO radio channels based on NLoS indoor measurements," *IEEE Trans. Veh. Technol.*, vol. 53, no. 3, pp. 655–665, May 2004.
- [3] D.-S. Shiu, G. J. Foschini, M. J. Gans, and J. M. Kahn, "Fading correlation and its effect on the capacity of multielement antenna systems," *IEEE Trans. Commun.*, vol. 48, no. 3, pp. 502–513, Mar. 2000.
- [4] S. A. Jafar and A. Goldsmith, "Transmitter optimization and optimality of beamforming for multiple antenna systems," *IEEE Trans. Wireless Commun.*, vol. 3, no. 4, pp. 1165–1175, Jul. 2004.
- [5] E. A. Jorswieck and H. Boche, "Channel capacity and capacity-range of beamforming in MIMO wireless systems under correlated fading with covariance feedback," *IEEE Trans. Wireless Commun.*, vol. 3, no. 5, pp. 1543–1553, Sep. 2004.
- [6] A. M. Tulino, A. Lozano, and S. Verdu, "Impact of antenna correlation on the capacity of multiantenna channels," *IEEE Trans. Inf. Theory*, vol. 51, no. 7, pp. 2491–2509, Jul. 2005.
- [7] W. Chang, S. Chung, and Y. H. Lee, "Diversity-multiplexing tradeoff in rank-deficient and spatially correlated MIMO channels," in *IEEE International Symposium on Information Theory (ISIT)*, Jul. 2006, pp. 1144–1148.
- [8] E. Dall'Anese, A. Assalini, and S. Pupolin, "On the effect of imperfect channel estimation upon the capacity of correlated MIMO fading channels," in *IEEE Vehicular Technology Conference*, Apr. 2009, pp. 1–5
- [9] A. Soysal, "Tightness of capacity bounds in correlated MIMO systems with channel estimation error," in *IEEE International Symposium on Personal, Indoor and Mobile Radio Communications*, Sep. 2010, pp. 667–671.
- [10] M. Dai, B. Clerckx, D. Gesbert, and G. Caire, "A rate splitting strategy for massive MIMO with imperfect CSIT," *IEEE Trans. Wireless Commun.*, vol. 15, no. 7, pp. 4611–4624, 2016.
- [11] Hyundong Shin and Jae Hong Lee, "Capacity of multiple-antenna fading channels: spatial fading correlation, double scattering, and keyhole," *IEEE Trans. Inf. Theory*, vol. 49, no. 10, pp. 2636–2647, 2003.
- [12] A. Abdi and M. Kaveh, "A space-time correlation model for multielement antenna systems in mobile fading channels," *IEEE J. Sel. Areas Commun.*, vol. 20, no. 3, pp. 550–560, 2002.
- [13] J.-. Lee, J.-. Ko, and Y.-. Lee, "Effect of transmit correlation on the sumrate capacity of two-user broadcast channels," *IEEE Trans. Commun.*, vol. 57, no. 9, pp. 2597–2599, Sep. 2009.
- [14] J. W. Lee, H. N. Cho, H. J. Park, and Y. H. Lee, "Sum-rate capacity of correlated multi-user MIMO channels," in *Information Theory and Applications Workshop (ITA)*, Jan. 2010, pp. 1–5.
- [15] T. Al-Naffouri, M. Sharif, and B. Hassibi, "How much does transmit correlation affect the sum-rate scaling of MIMO Gaussian broadcast channels?" *IEEE Trans. Commun.*, vol. 57, no. 2, pp. 562–572, Feb. 2009.
- [16] A. Abdi and M. Kaveh, "A space-time correlation model for multielement antenna systems in mobile fading channels," *IEEE J. Sel. Areas Commun.*, vol. 20, no. 3, pp. 550–560, Apr. 2002.
- [17] J. Nam, J. Y. Ahn, A. Adhikary, and G. Caire, "Joint spatial division and multiplexing: Realizing massive MIMO gains with limited channel state information," in 46th Annual Conference on Information Sciences and Systems (CISS), Mar. 2012, pp. 1–6.
- [18] J. Nam, "Fundamental limits in correlated fading MIMO broadcast channels: Benefits of transmit correlation diversity," in *IEEE International* Symposium on Information Theory (ISIT), Jun. 2014, pp. 2889–2893.
- [19] J. Nam, A. Adhikary, J. Y. Ahn, and G. Caire, "Joint spatial division and multiplexing: Opportunistic beamforming, user grouping and simplified downlink scheduling," *IEEE J. Sel. Topics Signal Process.*, vol. 8, no. 5, pp. 876–890, Oct. 2014.
- [20] J. Nam, G. Caire, and J. Ha, "On the role of transmit correlation diversity in multiuser MIMO systems," *IEEE Trans. Inf. Theory*, vol. 63, no. 1, pp. 336–354, Jan. 2017.
- [21] A. Adhikary and G. Caire, "JSDM and multi-cell networks: Handling inter-cell interference through long-term antenna statistics," in 48th Asilomar Conference on Signals, Systems and Computers, Nov. 2014, pp. 649–655.
- [22] A. Adhikary, H. S. Dhillon, and G. Caire, "Massive-MIMO meets HetNet: Interference coordination through spatial blanking," *IEEE J. Sel. Areas Commun.*, vol. 33, no. 6, pp. 1171–1186, Jun. 2015.
- [23] A. Adhikary, E. A. Safadi, and G. Caire, "Massive MIMO and intertier interference coordination," in *Information Theory and Applications Workshop (ITA)*, Feb. 2014, pp. 1–10.

- [24] B. Hassibi and B. M. Hochwald, "How much training is needed in multiple-antenna wireless links?" *IEEE Trans. Inf. Theory*, vol. 49, no. 4, pp. 951–963, Apr. 2003.
- [25] F. Zhang, M. Fadel, and A. Nosratinia, "Spatially correlated MIMO broadcast channel: Analysis of overlapping correlation eigenspaces," in *IEEE International Symposium on Information Theory (ISIT)*, Jun. 2017, pp. 1097–1101.
- [26] K.-H. Ngo, S. Yang, and M. Guillaud, "An achievable DoF region for the two-user non-coherent MIMO broadcast channel with statistical CSI," in 2017 IEEE Information Theory Workshop (ITW), Nov. 2017, pp. 604–608.
- [27] F. Zhang and A. Nosratinia, "Spatially correlated MIMO broadcast channel with partially overlapping correlation eigenspaces," in 2018 IEEE International Symposium on Information Theory (ISIT), Jun. 2018, pp. 1520–1524.
- [28] K.-H. Ngo, F. Zhang, S. Yang, and A. Nosratinia, "Two-user MIMO broad-cast channel with transmit correlation diversity: Achievable rate regions," in 2021 IEEE Information Theory Workshop (ITW), Kanazawa, Japan, 2021.
- [29] L. Zheng and D. N. C. Tse, "Communication on the Grassmann manifold: A geometric approach to the noncoherent multiple-antenna channel," *IEEE Trans. Inf. Theory*, vol. 48, no. 2, pp. 359–383, Feb. 2002.
- [30] M. Chiani, M. Z. Win, and A. Zanella, "On the capacity of spatially correlated MIMO Rayleigh-fading channels," *IEEE Trans. Inf. Theory*, vol. 49, no. 10, pp. 2363–2371, Oct. 2003.
- [31] E. M. Luks, F. Rákóczi, and C. R. Wright, "Some algorithms for nilpotent permutation groups," *J. Symb. Comput.*, vol. 23, no. 4, pp. 335–354, Apr. 1997. [Online]. Available: http://dx.doi.org/10.1006/jsco.1996.0092
- [32] H. Joudeh and B. Clerckx, "Robust transmission in downlink multiuser MISO systems: A rate-splitting approach," *IEEE Trans. Signal Process*, vol. 64, no. 23, pp. 6227–6242, Dec. 2016.
- [33] Z. Li, C. Ye, Y. Cui, S. Yang, and S. Shamai, "Rate splitting for multiantenna downlink: Precoder design and practical implementation," *IEEE J. Sel. Areas Commun.*, vol. 38, no. 8, pp. 1910–1924, Jun. 2020.
- [34] Y. Li and A. Nosratinia, "Product superposition for MIMO broadcast channels," *IEEE Trans. Inf. Theory*, vol. 58, no. 11, pp. 6839–6852, Nov. 2012.
- [35] —, "Coherent product superposition for downlink multiuser MIMO," IEEE Trans. Wireless Commun., vol. 14, no. 3, pp. 1746–1754, Mar. 2015.
- [36] F. Zhang, K.-H. Ngo, S. Yang, and A. Nosratinia, "Transmit correlation diversity: Generalization, new techniques, and improved bounds," arXiv Preprint arXiv:2104.09711.
- [37] M. Fadel and A. Nosratinia, "Coherence disparity in broadcast and multiple access channels," *IEEE Trans. Inf. Theory*, vol. 62, no. 12, pp. 7383–7401, Dec. 2016.
- [38] A. El Gamal and Y.-H. Kim, Network Information Theory. New York, NY, USA: Cambridge University Press, 2011.
- [39] R. Diestel, Graph Theory: 5th edition, ser. Springer Graduate Texts in Mathematics. Springer-Verlag, © Reinhard Diestel, 2017.
- [40] M. R. Garey and D. S. Johnson, Computers and Intractability; A Guide to the Theory of NP-Completeness. New York, NY, USA: W. H. Freeman & Co., 1990.
- [41] E. Björnson, J. Hoydis, and L. Sanguinetti, "Massive MIMO networks: Spectral, energy, and hardware efficiency," Foundations and Trends® in Signal Processing, vol. 11, no. 3-4, pp. 154–655, 2017. [Online]. Available: http://dx.doi.org/10.1561/2000000093
- [42] Z. Jiang, A. F. Molisch, G. Caire, and Z. Niu, "Achievable rates of FDD massive MIMO systems with spatial channel correlation," *IEEE Trans. Wireless Commun.*, vol. 14, no. 5, pp. 2868–2882, 2015.
- [43] G. Caire, N. Jindal, M. Kobayashi, and N. Ravindran, "Multiuser MIMO achievable rates with downlink training and channel state feedback," *IEEE Trans. Inf. Theory*, vol. 56, no. 6, pp. 2845–2866, 2010.
- [44] M. Ding and S. D. Blostein, "Maximum mutual information design for MIMO systems with imperfect channel knowledge," *IEEE Trans. Inf. Theory*, vol. 56, no. 10, pp. 4793–4801, 2010.

Fan Zhang (Student Member, IEEE) received the B.S. degree in electrical engineering from Peking University, Beijing, China, the M.S. degree and Ph.D. degree in electrical engineering from the University of Texas at Dallas, Richardson, Texas, USA. His research interests include information theory and wireless communication, with emphasis on coherence diversity.

Khac-Hoang Ngo (Member, IEEE) received the B.Eng. degree (Hons.) in electronics and telecommunications from University of Engineering and Technology, Vietnam National University, Hanoi, Vietnam, in 2014; and the M.Sc. degree (Hons.) and Ph.D. degree in wireless communications from CentraleSupélec, Paris-Saclay University, France, in 2016 and 2020, respectively. His Ph.D. thesis was also realized at Mathematical and Algorithmic Sciences Laboratory, Paris Research Center, Huawei Technologies France. Since September 2020, he has been working as a postdoctoral researcher at Communication Systems Group, Department of Electrical Engineering, Chalmers University of Technology, Sweden. He is also an adjunct lecturer at University of Engineering and Technology, Vietnam National University Hanoi, Vietnam. His research interests include wireless communications and information theory, with an emphasis on massive random access, edge computing, MIMO, noncoherent communications, coded caching, and network coding. He received the Honda Award for Young Engineers and Scientists (Honda Y-E-S Award) in Vietnam in 2013, the Marie Skłodowska-Curie Actions (MSCA) Individual Fellowship in 2021, and the 2021 "Signal, Image & Vision Ph.D. Thesis Prize" by Club EEA, GRETSI and GdR-ISIS, France.

Sheng Yang (Member, IEEE) received the B.E. degree in electrical engineering from Jiaotong University, Shanghai, China, in 2001, and both the engineer degree and the M.Sc. degree in electrical engineering from Telecom ParisTech, Paris, France, in 2004, respectively. In 2007, he obtained his Ph.D. from Université de Pierre et Marie Curie (Paris VI). From October 2007 to November 2008, he was with Motorola Research Center in Gif-sur-Yvette, France, as a senior staff research engineer. Since December 2008, he has joined CentraleSupélec, Paris-Saclay University, where he is currently a full professor. From April 2015, he also holds an honorary associate professorship in the department of electrical and electronic engineering of the University of Hong Kong (HKU). He received the 2015 IEEE ComSoc Young Researcher Award for the Europe, Middle East, and Africa Region (EMEA). He was an associate editor of the IEEE transactions on wireless communications from 2015 to 2020. He is currently an associate editor of the IEEE transactions on information theory.

Aria Nosratinia (Fellow, IEEE) is Erik Jonsson Distinguished Professor and associate head of the electrical and computer engineering department at the University of Texas at Dallas. He received his Ph.D. in Electrical and Computer Engineering from the University of Illinois at Urbana-Champaign in 1996. He has held visiting appointments at Princeton University, Rice University, and UCLA. His interests lie in the broad area of information theory and signal processing, with applications in wireless communications, machine learning, and data security and privacy. Dr. Nosratinia is a fellow of IEEE for contributions to multimedia and wireless communications. He has served as editor and area editor for the IEEE Transactions on Wireless Communications, and editor for the IEEE Transactions on Information Theory, IEEE Transactions on Image Processing, IEEE Signal Processing Letters, IEEE Wireless Communications (Magazine), and Journal of Circuits, Systems, and Computers. He has received the National Science Foundation career award, and the outstanding service award from the IEEE Signal Processing Society, Dallas Chapter. He has served as the secretary of the IEEE information theory society, treasurer for ISIT, publications chair for the IEEE Signal Processing Workshop, as well as member of the technical committee for a number of conferences. He was the general co-chair of IEEE Information Theory Workshop in 2018. Dr. Nosratinia has been named a highly cited researcher by Clarivate Analytics.